

Hydroxy amino acids in carbonaceous chondrites and their formation mechanisms

古賀, 俊貴

<https://hdl.handle.net/2324/4474944>

出版情報 : Kyushu University, 2020, 博士 (理学), 課程博士
バージョン :
権利関係 :

**Hydroxy amino acids in carbonaceous chondrites
and their formation mechanisms**

Toshiki Koga

Department of Earth and Planetary Sciences
Faculty of Science
Kyushu University

Abstract

Carbonaceous chondrites contain a variety of extraterrestrial amino acids, which were formed throughout the processes from the interstellar medium to the meteorite parent body. The abiotically synthesized amino acids can provide us information for understanding the chemical evolution of biological-related compounds and possibly the emergence of life on the early Earth. The molecular distributions and enantiomeric excesses of meteoritic amino acids have been thoroughly investigated in various types of carbonaceous chondrites over half a century. Recently, a family of C₃ and C₄ hydroxy amino acids (HAAs) was newly identified in the CM2 Murchison meteorite. However, the distributions and enantiomeric compositions of HAAs remained unknown in other carbonaceous chondrites.

This thesis consists of three chapters, as followed.

Chapter 1: The abundances, distributions, and enantiomeric ratios of C₃ and C₄ HAAs were investigated in five CM chondrites and four CR chondrites by gas chromatography/mass spectrometry (GC-MS) analyses. A new GC-MS analytical technique was developed to be capable of analyzing 13 different HAAs in a single run. The HAA analyses performed in this study revealed that 1) the petrographic type CR2 chondrites contained greater abundances of α -HAAs than CM chondrites and 2) the hot water and HCl extracts of CM and CR chondrites contained roughly similar ranges of abundances of β - and γ -HAAs. Application of the GC-MS method developed here resulted in the first successful chromatographic resolution of the enantiomers of an α -dialkyl HAA, D,L- α -methylserine, in carbonaceous chondrites. Meteoritic α -methylserine was found to be mostly racemic within error and did not show L-enantiomeric excesses correlating with the degree of aqueous alteration, a phenomenon

observed in meteoritic isovaline, another α -dialkyl amino acid. It is considered that HAAs in CM and CR chondrites could have been produced from the Strecker cyanohydrin reaction (for α -HAAs) and an ammonia-involved formose-like reaction (for β -, and γ -HAAs).

In Chapter 2, an amino acid synthesis experiment from glycolaldehyde and ammonia was performed to reveal amino acid formation pathways by the ammonia-involved formose-like reaction. This experiment was conducted under air or nitrogen atmosphere to evaluate the effects of free oxygen for the amino acid synthesis in the reaction. The reaction products were analyzed by GC/MS to compare the distributions of synthesized organic compounds between the different conditions. As a result, oxygen in the air promoted the syntheses of amino acids and sugar acids, indicating oxidation was involved in their formation mechanisms. A precursor compound of glycine was identified as N-oxalylglycine that can be synthesized from ammonia and glyoxylic acid, which was produced by glycolaldehyde oxidation. The formation mechanism of glycine in this experiment could be generalized as the reaction of an oxoacid and ammonia; thus, it can be hypothesized that the reactions of α -, β -, and γ -oxo acids with ammonia could produce various structural isomers of amino acids, including α -, β -, and γ -HAAs.

In Chapter 3, the results and discussion obtained from the amino acid synthesis experiments were compared with the HAA distributions of the CM and CR chondrites and observations in the previous studies. This study suggests that the ammonia-involved formose-like reaction could complement previously proposed formation mechanisms such as the Strecker-cyanohydrin reaction to explain the distribution of meteoritic HAAs.

Acknowledgements

This thesis consists of two Organic Geochemistry & Cosmochemistry Laboratory in the Department of Earth and Planetary Sciences, Graduate School of Science, Kyushu University and Astrobiology Analytical Laboratory in NASA's Goddard Space Flight Center. I am deeply grateful to my supervisor, Prof. Hiroshi Naraoka, for years of his uncountable support, guidance, and encouragement since I was an undergraduate student. I would like to express my gratitude to Dr. Jason P. Dworkin and Dr. Daniel P. Glavin for allowing me to conduct research activities at NASA's Goddard Space Flight Center. I would like to thank Dr. Jamie E. Elsila for her support in obtaining Antarctic meteorite samples for my research. I am deeply grateful to Dr. Hannah L. McLain, Dr. Jason L. McLain, and their children for warmly welcoming me into their home when I was in the U.S. I would like to show my appreciation to Dr. Eric. T. Parker, for his numerous advice and comments, to improve the manuscript and my capability as a researcher. I would like to thank Dr. José C. Aponte, Dr. Danielle N. Simkus, and Dr. Heather V. Graham for their advice and support in conducting experiments and analyses at the laboratory. I would like to thank Assoc. prof. Noriaki Yamauchi and Prof. Takaaki Noguchi at Kyushu University for their constructive advice and comments in the discussion. I acknowledge support by all faculty members at Kyushu University and NASA's Goddard Space Flight Center. Last of all, I am grateful to the past and present members of the Organic Geochemistry & Cosmochemistry Laboratory and my family for their encouragement.

List of Figures

- Fig. 1-1.** Plausible formation mechanisms for α -, β -, γ -, and δ -amino acids..... 23
- Fig. 1-2.** All the structural isomers of C_3 and C_4 hydroxy amino acids investigated in this study..... 24
- Fig. 1-3.** The selected regions of the GC-MS extracted ion chromatograms of the C_3 and C_4 hydroxy amino acids in the HW extracts of the CM and CR chondrites studied here. 25
- Fig. 1-4.** The selected regions of the GC-MS extracted ion chromatograms of the C_3 and C_4 hydroxy amino acids in the 6 M HCl extracts of the CM and CR chondrites studied here. 26
- Fig. 1-5.** The relative abundances of C_3 and C_4 hydroxy amino acids in CM and CR carbonaceous chondrites for A) the HW extracts, B) the HCl extracts, and C) the combined (HW + HCl) extracts..... 27
- Fig. 1-6.** Examples of the proposed synthetic pathways for the formation of select α -hydroxy amino acids via the Strecker cyanohydrin reaction..... 28
- Fig. 1-7.** The recombination of select free radical pairs to form carbonyl compounds, which serve as precursors for forming C_3 and C_4 α -hydroxy amino acids. 29
- Fig. 2-1.** A schematic diagram of the amino acid synthesis experiment conducted in this study. A glass ampoule was sealed under air or nitrogen atmosphere to evaluate the effect of oxygen for the syntheses of organic compounds, including amino acids. 45
- Fig. 2-2.** A comparison of the 10–40 min regions of the GC-MS total ion chromatograms (m/z 50–510) obtained from the non-hydrolyzed (A) air- and (B) N_2 -products. 46
- Fig. 2-3.** A comparison of the molar ratios of amino acids in the air- and N_2 -products relative to starting glycolaldehyde..... 47

Fig. 2-4. Comparisons of the 10–41 min regions of the GC-MS extracted ion chromatograms of the base peaks of the isopropyl-ester derivatized (A) ^{13}C -labeled air-product (m/z 105) and (B) commercial standard ^{12}C -N-oxalylglycine (m/z 102) and their mass spectrums (m/z 50–250)..... 48

Fig. 2-5. The plausible formation pathway of glycine from glycolaldehyde and ammonia via the synthesis of N-oxalylglycine under alkaline condition..... 49

Fig. 2-6. The possible formation pathways of α -, β -, and γ -amino acids from the corresponding oxoacids and ammonia based on the formation of glycine from glyoxylic acid and ammonia..... 50

List of Tables

Table 1-1. Meteorite samples analyzed in this study.	30
Table 1-2. Summary of the average abundances (nmol/g) of the three- to four-carbon hydroxy amino acids identified in the HW and HCl extracts of CM carbonaceous chondrites measured by GC-MS ^a	31
Table 1-3. Summary of the average abundances (nmol/g) of the three- to four-carbon hydroxy amino acids identified in the HW and HCl extracts of CR carbonaceous chondrites measured by GC-MS ^a	32
Table 1-4. Summary of the combined abundances (nmol/g) of the three- to four-carbon hydroxy amino acids in the two extracts (HW + HCl extracts) of CM and CR carbonaceous chondrites measured by GC-MS ^a	33
Table 1-5. Summary of D/L ratios and L-enantiomeric excesses (L_{ee}) measured for several α -hydroxy amino acids in the HW and HCl extracts of CM and CR chondrites ^a	34
Table 2-1. The concentrations of amino acids relative to starting glycolaldehyde (ppm by mol) in the non-hydrolyzed (free) and 6 M HCl hydrolyzed (total) air- and N ₂ products ^a	51
Table 3-1. The abundance ratios of serine to isoserine in the CM and CR chondrites and the experimental products from glycolaldehyde and ammonia ^a	56
Table S1. Summary of the fragment ions (m/z) used for quantification of each HAA in the CM and CR chondrites.	63

Contents

Chapter 1. Hydroxy Amino Acids in CM and CR Chondrites	1
1.1. Introduction	1
1.2. Materials and Methods	6
1.2.1. Chemicals and Reagents	6
1.2.2. Meteorite Samples and Sample Preparation	7
1.2.3. GC-MS Analysis	8
1.3. Results and Discussion	10
1.3.1. Analytical Performance of the Developed Method	10
1.3.2. Hydroxy Amino Acid Abundances	10
1.3.3. Enantiomeric Compositions of Non-Proteinogenic Hydroxy Amino Acids	13
1.3.4. A Proposed Formation Mechanism for Prominent α -Hydroxy Amino Acids: Strecker-Cyanohydrin Synthesis	15
1.3.5. A Proposed Formation Mechanism for β -, and γ -Hydroxy Amino Acids: Ammonia-Involved Formose-like Reaction	18
1.4. Conclusion	21
1.5. Figures	23
1.6. Tables	30
Chapter 2. The Amino Acid Syntheses from Glycolaldehyde and Ammonia	35
2.1. Introduction	35
2.2. Materials and Methods	36
2.2.1. Chemicals and Reagents	36
2.2.2. Experimental Amino Acid Synthesis and Sample Preparation	37
2.2.3. GC-MS Analysis	38
2.3. Results and Discussion	40
2.3.1. A Comparison of Molecular Distributions between the Air- and N ₂ - Products	40

2.3.2. A Detection of ¹³ C-Labeled N-Oxalylglycine in the Air-Product.	41
2.3.3. The Formation Pathway of Glycine via N-Oxalylglycine: Implications for Amino Acid Syntheses by the Ammonia-Involved Formose-like Reaction.	42
2.4. Conclusion.....	44
2.5. Figures.....	45
2.6. Tables.....	51
Chapter 3. Amino Acid Syntheses from Glycolaldehyde and Ammonia in the Meteorite Parent Bodies	52
3.1. Tables.....	56
References.....	57
Supplementary Information	63

Chapter 1.

Hydroxy Amino Acids in CM and CR Chondrites

1.1. Introduction

Carbonaceous chondrites preserve primitive materials in the early solar system over the past 4.5 billion years, including organic matter that consists of insoluble macromolecules (insoluble organic matter; IOM) and lower-molecular-weight soluble compounds (soluble organic matter; SOM) (Pizzarello, S.; Cooper, G. W.; Flynn 2006). The most intriguing SOM is extraterrestrial amino acids because of the building blocks of proteins common to all terrestrial life. The delivery of the meteoritic organic matter, including amino acids, could supply organic carbon to the early Earth that would have contributed to the emergence of life (Chyba and Sagan 1992). Besides, meteoritic amino acids are one of the abiotically synthesized products in natural environments throughout the early solar system formation.

One of the formation environments of meteoritic amino acids might be the meteorite parent body (planetesimal) that was formed by the accumulation of interstellar silicate core-mantle grains containing water ices and amino acids' precursor molecules (*e.g.*, carbonyl compounds, ammonia, and HCN) from the interstellar medium (Glavin et al. 2018). After incorporating into the meteorite parent body, the precursor compounds reacted with each other to produce amino acids in melted water by the heat from the decay of short-lived radionuclides (*e.g.*, ^{26}Al and ^{60}Fe) and impact shocks. The activity of water in meteorite parent bodies is recorded by aqueous alteration of meteoritic anhydride silicate minerals (*e.g.*, amorphous Mg–Fe silicate, olivine, and pyroxene) into secondary minerals (*e.g.*, phyllosilicates, oxides, and carbonates) (Kawasaki et al. 2006). Thus, historically, meteoritic amino acids have been mainly investigated in the aqueously altered carbonaceous chondrites, such as CM, CR, and CI chondrites (carbonaceous chondrites are classified into 8 chemical groups based on the elemental and isotopic isotope compositions) (Weisberg et al. 2006).

Since the detection of non-proteinogenic amino acids in the CM2 Murchison meteorite (*e.g.*, Kvenvolden et al., 1971), meteoritic amino acids have been extensively in a variety of carbonaceous chondrites (particularly CM, CR, and CI chondrites) over the last five decades. During this period, analytical methods for amino acids have continuously improved, enabling the ability to chromatographically separate amino acid structural isomers and enantiomers and to detect trace quantities of amino acids (Glavin et al. 2018 and references therein). By applying increasingly improved analytical techniques to study the amino acid chemistry of meteorites, new information has been revealed to suggest that the total amino acid abundances and the relative abundances of the C₅ amino acid isomers as a function of amine position (α , β , γ , or δ) are significantly different between unaltered and aqueously altered carbonaceous chondrites (Glavin and Dworkin 2009; Glavin et al. 2006, 2010, 2020a). For example, the unaltered or moderately altered carbonaceous chondrites (*e.g.*, CM2, CR2, and CR3) possess larger total amino acid abundances (~100 ppm) and an amino acid distribution that is dominated by α -amino acids (Elsila et al. 2016 and references therein). In contrast, the heavily altered chondrites (*e.g.*, CI1, CM1, and CR1) possess smaller total amino acid abundances (~1–7 ppm) and greater relative abundances of β -, γ -, and δ -amino acids (Elsila et al. 2016 and references therein). Thus, it has been considered that the total amino acid abundances and the distribution of structural isomers could provide insight into the formation mechanisms of meteoritic amino acids and the possible processing histories of the meteorite parent bodies, especially relating to the degree of aqueous alteration (Elsila et al. 2016 and references therein).

It has also been hypothesized that the extent to which meteorite parent bodies have undergone aqueous alteration may correspond to observed L-enantiomeric excesses of extraterrestrial amino acids. Many amino acids possess a property known as chirality, whereby the chemical compound is composed of two non-superimposable mirror-image structures or enantiomers. These enantiomers are distinguished as the so-called L-amino acids (“left-

handed”) or D-amino acids (“right-handed”). Terrestrial life uses L-enantiomers almost exclusively as a component of proteins, whereas abiotically synthesized amino acids contain an equal mixture (racemic) of both enantiomers. Therefore, chirality is a critical amino acid property to monitor when assessing the origins of these biomolecules. An example of a meteoritic amino acid that is a useful target analyte to evaluate potential enantiomeric excesses is the non-proteinogenic amino acid, isovaline, which is rare or non-existent in biology (Elsila et al. 2012; Glavin and Dworkin 2009). Different laboratories have reported that isovaline has various L-enantiomeric excesses ranging from 0 % to ~20 %, with an increase in enantiomeric excess roughly correlating with an increased degree of aqueous alteration among the carbonaceous chondrites analyzed (Elsila et al. 2016 and references therein). More specifically, unaltered type 3 carbonaceous chondrites show racemic isovaline, but more aqueously altered type 2 or type 1 carbonaceous chondrites contain L-isovaline excesses (Glavin and Dworkin 2009; Glavin et al. 2010, 2020b, 2020a; Martins et al. 2015; Pizzarello et al. 2003).

Several formation mechanisms for meteoritic amino acids have been suggested to explain the synthesis of each structural isomer as a function of amine position (α , β , γ , or δ). Firstly, α -amino acids could be produced from the Strecker-cyanohydrin reaction (**Fig. 1-1**). In the reaction, the starting carbonyl compounds (aldehyde or ketone) react with ammonia (NH_3) to form imines, followed by the addition of cyanide (CN^-) and the hydrolysis of the α -aminonitriles, resulting in α -amino acids. The carbonyl compounds can also react with cyanide, instead of ammonia, to form α -cyanohydrins hydrolyzed to yield α -hydroxy acids. Besides, when the carbonyl compounds react with an amino group ($-\text{NH}_2$) of α -amino acids, the α -iminodicarboxylic acids can be produced byproducts in the Strecker-cyanohydrin synthesis. Here, the CM2 Murchison meteorite has been reported to contain predominant α -amino acids with the coexistence of α -hydroxy acids and α -iminodicarboxylic acids (Lerner and Cooper 2005; Peltzer and Bada 1978; Peltzer et al. 1984), indicating that the Strecker-cyanohydrin synthesis proceeded to produce α -amino acids in the Murchison meteorite parent body.

Recently, a site-specific carbon isotopic analysis of DL-alanine in the Murchison meteorite also indicated the significant contribution of the Strecker-cyanohydrin synthesis for producing straight-chain α -amino acids in the meteorite from ^{13}C -enriched aldehydes, ammonia, and ^{13}C -depleted cyanide (Chimiak et al. 2021). Therefore, the predominant α -amino acids in the less aqueously altered CM and CR chondrites have been considered to be yielded by the Strecker-cyanohydrin synthesis as proposed for the CM2 Murchison meteorite (Aponte et al. 2017; Elsila et al. 2016). Secondly, β -amino acids can be synthesized by the Michael addition of ammonia to α , β -unsaturated nitriles followed by hydrolysis of the products (Ehrenfreund et al. 2001; Glavin et al. 2010) (**Fig. 1-1**). Thirdly, γ - and δ -amino acids can be produced by the thermal decarboxylation of α -amino dicarboxylic acids or the hydrolysis of lactams (Cooper and Cronin 1995). In contrast to the less aqueously altered chondrites (*e.g.*, types 3 and 2) that contained the predominant α -amino acid isomers, the heavily altered chondrites (*e.g.*, CI1, CM1, and CR1) possessed greater relative abundances of β -, γ -, and δ -amino acids (Glavin et al. 2006, 2010). In either scenario, amino acid syntheses and degradations require the activity of water. Therefore, the aqueous alteration of meteorite parent bodies is thought to play a crucial role in influencing the distribution of meteoritic amino acids (Botta and Bada 2002; Elsila et al. 2016).

While these formation mechanisms could respectively explain the distribution of α -, β -, γ -, and δ -amino acids in unaltered and aqueously altered chondrites, it remains unclear whether the diversity of meteoritic amino acids could be derived from a comprehensive formation mechanism that can simultaneously explain the formation of various amino acid isomers. To explore such a formation mechanism, we conducted an amino acid synthesis experiment from aldehydes (formaldehyde, glycolaldehyde, and acetaldehyde) and ammonia in aqueous solution by heating at 60 °C for 6 days (Koga and Naraoka 2017). As a result, 17 amino acids were identified, including glycine, alanine, β -alanine (conventional amino acids found in carbonaceous chondrites), and C₃ and C₄ hydroxy amino acids (HAAs) (hydroxyl (–

OH) group-bearing amino acids) with their α -, β -, and γ -structural isomers. Although aliphatic amino acids have been thoroughly investigated in carbonaceous chondrites, HAAs have been understudied except for proteinogenic amino acids serine and threonine. Thus, we investigated the HAA distribution in the water and hydrochloric acid (HCl) extracts of the Murchison meteorite and detected nine newly identified C₃ and C₄ HAAs with α -, β -, and γ -amino positions (**Fig. 1-2**), most of which were produced from aldehydes and ammonia in the performed experiments (Koga and Naraoka 2017). It is worth noting that HAAs were detected not only in the acid hydrolysates of the hot water extracts but were also present at comparable or greater abundances in the 6 M HCl extracts of the meteorite residues that had previously experienced hot water extraction. There have been limited efforts to detect and quantify amino acids in aqueous HCl extracts of meteorites (Bada et al. 1998; Engel and Nagy 1982; Glavin et al. 1999, Koga and Naraoka, 2017). What has been learned from investigating the aqueous HCl extract of the Murchison meteorite is that HAAs represent a new subclass of meteoritic amino acids that are not necessarily released from the meteorite matrix by hot water extraction (Koga and Naraoka, 2017). However, it remains unknown if abundances and distributions of structural isomers of HAAs exist in carbonaceous chondrites other than CM2 Murchison meteorite. Moreover, enantiomeric analyses of HAAs by gas chromatography/mass spectrometry (GC-MS) have been limited in previous studies, except for serine and threonine (Pizzarello et al. 2012). In this study, we developed a new GC-MS method to investigate the abundances of three- and four-carbon (C₃-C₄) HAA structural isomers and the enantiomeric excesses of HAAs in CM and CR chondrites ranging from type 1 to type 2, to evaluate the molecular distributions of HAAs across a range of different carbonaceous chondrites.

1.2. Materials and Methods

1.2.1. Chemicals and Reagents

Commercial standards of HAAs were purchased from various manufacturers as follows: Sigma-Aldrich: D,L- α -methylserine (>99 % purity), D-threonine (>98 % purity), L-threonine (>98 % purity), D,L-*allo*-threonine (>99 % purity), D,L-isoserine (>98 % purity), D,L-homoserine (>99 % purity), D- β -homoserine (>99 % purity), L- β -homoserine (>99 % purity), TCI: D,L-4-amino-3-hydroxybutanoic acid (4-A-3-HBA) (>98 % purity), Enamine Ltd.: a combined D,L-isothreonine and D,L-*allo*-isothreonine standard (>95 % purity), and Fluka: D,L-serine (>99 % purity). Racemic standards for 3-amino-2-(hydroxymethyl)propanoic acid (3-A-2-HMPA) and 4-amino-2-hydroxybutanoic acid (4-A-2-HBA) were not commercially available, so the following enantiopure standards of these amino acids were purchased from Sigma-Aldrich: D-3-A-2-HMPA (>96 % purity) and L-4-A-2-HBA (>96 % purity). The D,L- α -methylisoserine standard was obtained by hydrolysis of D,L-methyl 3-amino-2-hydroxy-2-methylpropanoate hydrochloride (>97 % purity, Aurum Pharmatech LLC) via 6 M HCl vapor hydrolysis at 150 °C for 3 h. A stock mixed HAA solution (~8 μ M per analyte) was prepared by combining individual HAA standards described above in Milli-Q ultrapure water (18.2 M Ω , <3 ppb total organic carbon). As an internal standard, a stock solution of 8-aminooctanoic acid (8-AOA) (>99 %, Sigma Aldrich) was prepared with the same concentration (~8 μ M).

All glassware and sample handling tools were rinsed with Milli-Q ultrapure water, wrapped in aluminum foil, and then heated at 500 °C, in air, overnight. Preparation of reagents used to perform acid-vapor hydrolysis (Glavin et al. 2006) and desalting by cation exchange chromatography (Glavin et al. 2006; Simkus et al. 2019) are described elsewhere. Pre-column derivatization of samples before GC-MS analyses involved the use of acetyl chloride (Acros Organics, 99+ %), isopropanol (Sigma-Aldrich, 99+ %), heptafluorobutyric anhydride (HFBA, Sigma-Aldrich, \geq 98 %), and chloroform (Sigma-Aldrich, for HPLC, \geq 99.9 %).

1.2.2. Meteorite Samples and Sample Preparation

The interior chips of five CM and four CR chondrites, none of which contained visible evidence of fusion crusts, were used for HAA analyses in this study (**Table 1**). The Antarctic CM2 chondrites of Asuka 881458 (A-881458) and Yamato 791198 (Y-791198) were provided by the National Institute of Polar Research (NIPR), Japan. The other Antarctic CM2 chondrites Lewis Cliffs (LEW) 90500 and Lonewolf Nunataks (LON) 94101, the CM 1/2 chondrite Allan Hills (ALH) 83100, the CR2 chondrite Miller Range (MIL) 07525, the CR2 chondrites Meteorite Hills (MET) 00426 and LaPaz Icefield (LAP) 02342, and the CR1 chondrite Grosvenor Mountains (GRO) 95577 were all provided by the Antarctic meteorite curator at the NASA Johnson Space Center. The subtypes of these carbonaceous chondrites were suggested by several previous studies, as summarized in **Table 1-1**. In this study, the CR chondrite subtype classifications were implemented as described by Harju et al. (2014), Howard et al. (2015), and Alexander et al. (2013) (*e.g.*, LAP 02332 (CR2.8/2.7/2.5)). The CM chondrite subtype classifications were implemented as described by Howard et al. (2015) and Alexander et al. (2013) (*e.g.*, Y-791198 (CM1.6/1.5)). Although the subtype for A-881458 was not available, this meteorite has been classified as a very weakly heated CM2 chondrite (Kimura et al. 2011).

Each meteorite chip was separately crushed into a fine powder using ceramic mortars and pestles inside a positive pressure ISO 5 HEPA filtered laminar flow hood. A portion of each powdered sample (mass ~ 0.14–0.36 g, **Table 1-1**) was flame-sealed separately in a glass ampoule with 1 mL of Milli-Q ultrapure water and extracted at 100 °C for 24 h (hereafter referred to “Hot Water (HW) extraction”). Half of the HW extract supernatants were subjected to a 6 M doubly distilled HCl (ddHCl) vapor hydrolysis procedure at 150 °C for 3 h to determine total hydrolyzable amino acid content (Glavin et al. 2006). Upon completion of acid vapor hydrolysis, the HW extracts were dried under vacuum to remove excess HCl. After completing the HW extraction, the sample residues were then subjected to a second extraction

procedure using 6 M ddHCl at 105 °C for 24 h (hereafter referred to “HCl extraction”). The supernatants of the HCl extracts were then dried to a residue and set aside until further processing.

Once the supernatants from both extraction procedures were dried to a residue, the residues from the HW and HCl extractions were then individually reconstituted in 1 mL of Milli-Q water before being desalted using cation-exchange chromatography. The reconstituted HW and HCl extracts were individually loaded onto separate AG 50W-X8, 100-200 mesh, hydrogen form cation-exchange chromatography columns and desalted as described in Simkus et al. (2019). The resultant desalted HW and HCl extract eluates were dried and reconstituted in 100 μ L of ultrapure water. Next, 30 μ L of each re-suspended meteorite extract and the HAA standard solution, were separately spiked with 10 μ L of the internal standard (8-AOA) before being dried and derivatized for HAA analyses using the following protocol: 1) esterification with 160 μ L of isopropanol and 40 μ L of acetyl chloride at 100 °C for 3 h, 2) acylation with 50 μ L of HFBA at 100 °C for 3 h, 3) removal of excess heptafluorobutyric acids using a stream of dry nitrogen, and 4) dissolution into 10 μ L of chloroform before injection into the GC-MS system for analysis. Procedural blanks composed of Milli-Q water were prepared using the identical extraction and processing protocols as the meteorite samples and analyzed to provide background-corrected abundance estimates of target analytes.

1.2.3. GC-MS Analysis

The HW and HCl extracts of the CM and CR chondrites were analyzed for HAA abundances, distributions, and enantiomeric ratios by GC-MS. The HFBA-isopropyl derivatives of HAAs were analyzed using a Thermo Trace GC and Thermo DSQII electron-impact quadrupole mass spectrometer. Chromatographic separation was achieved using a 5 m base-deactivated fused silica guard column (Restek) in series with two 25 m CP-Chirasil-Dex CB columns (Agilent), followed by two 25 m Chirasil L-Val columns (Agilent). A helium flow rate of 2.6 mL/min, and the following temperature program was employed during

chromatographic separation: initial oven temperature was 60 °C and was held for 2 min, followed by ramping at 20 °C/min to 75 °C and held for 40 min, followed by ramping at 20 °C/min to 120 °C, followed by ramping at 1 °C/min to 130 °C, and finally ramping at 3 °C/min to 200 °C and held for 2 min.

The GC-MS method applied in this study was optimized to separate the enantiomers of α -methylserine, an amino acid with the same α -dialkyl structure as isovaline, which has been observed to possess L-enantiomeric excesses in other meteorites (Elsila et al. 2016 and references therein). Hydroxy amino acids in carbonaceous chondrites were identified based on retention times and mass fragmentation patterns compared to those of commercial standards. To improve instrumental detection limits, we operated the mass spectrometer in single ion monitoring mode to observe the characteristic HAA fragment ions for each analyte. Quantification was performed using the fragment ions of a given analyte that did not experience coelution with potentially interfering ions when analyzing a given sample. This approach helped to improve the accuracy of the quantitative measurements reported here. Hence, depending on the presence of interfering ions, in many cases different fragment ions were used to quantify the same HAAs in different meteorite samples (*e.g.*, m/z 252 and m/z 466 for D,L- α -methylisoserine). A detailed overview of which fragment ions were selected for quantifying a given analyte in each sample is provided in **Table S1**. HAAs were quantified by comparing the procedural blank-subtracted mass chromatographic peak areas in the meteorite samples to those in the analytical standard analyzed on the same day. The HAA peak areas obtained from the meteorite samples, blanks, and standards were corrected based on the peak area of the 8-AOA internal standard to minimize analytical errors between each GC-MS analysis that was executed using different injection volumes (typical injection volumes ranged from 1–3 μ L).

1.3. Results and Discussion

1.3.1. Analytical Performance of the Developed Method

Fig. 1-3 and Fig. 1-4 show the extracted ion chromatograms of the HAA derivatives obtained from the HW and HCl extracts of each meteorite, the procedural blank, and an HAA standard. Most target chiral HAAs were enantiomerically resolved by this GC-MS method, except for α -methylisoserine and β -homoserine (**Fig. 1-3 and Fig. 1-4**). A slight chromatographic resolution was achieved for D,L-isoserine, but these peaks were not baseline-resolved. The enantiomers of isothreonine and *allo*-isothreonine were successfully separated by the developed method; however, the elution orders of the enantiomers for these species were not determined due to the lack of enantiopure standards.

Although chromatographic resolution of HAA structural isomers was achieved among the analytes in the HAA standard, select instances of coelution were observed between target HAA species and non-targeted, non-HAA species in some meteorites, due to the chemical complexities of the samples studied here. Non-proteinogenic C₄ HAAs were not detected in the procedural blank; however, trace quantities of the common biological contaminants, L-serine and L-threonine, were identified in the procedural blank. The abundances of L-serine and L-threonine in the procedural blank were subtracted when performing quantitative analyses of these species in samples. Many of the targeted C₃ and C₄ HAAs were detected in both the HW and HCl extracts, including α -methylisoserine, which has not previously been identified in meteorites due to the lack of an available standard (Koga and Naraoka 2017).

1.3.2. Hydroxy Amino Acid Abundances

The distributions and abundances of HAAs observed in the HW and HCl extracts of the CM chondrites are shown in **Table 1-2**. The total HAA content in each extract of the CM chondrites ranged from 2.43 ± 0.09 nmol/g in the HCl extract of ALH 83100 (CM1/2, CM2.1/1.2/1.1) to 74 ± 5 nmol/g in the HCl extract of Y-791198 (CM2, CM2.4/1.6/1.5). The

trend of combined HAA abundances in the two extracts (HW + HCl extracts) of CM chondrites follows the order of Y-791198 (CM2, CM2.4/1.6/1.5), 126 ± 5 nmol/g > A-881458 (CM2, very weakly heated), 15.2 ± 0.3 nmol/g > ALH 83100 (CM1/2, CM2.1/1.2/1.1), 9.8 ± 0.2 nmol/g > LON 94101 (CM2, CM2.6/1.3/1.8), 7.0 ± 0.5 nmol/g \approx LEW 90500 (CM2, CM2.4/1.4/1.6), 6.94 ± 0.09 nmol/g. It must be noted that the HW extract of ALH 83100 contained elevated abundances of L-serine (5.0 ± 0.2 nmol/g) and L-threonine (1.66 ± 0.06 nmol/g) relative to the total HAA abundances (7.4 ± 0.2 nmol/g). Consequently, the HW extract of ALH 83100 likely contained significant terrestrial contamination of L-serine and L-threonine. The similar L-serine's contamination was observed for the HCl extract of LON 94101 (L-serine: 2.1 ± 0.5 nmol/g and the total abundance: 4.5 ± 0.5 nmol/g). If these likely L-contaminants are excluded from the total HAA sum, the observed trend in total HAA abundances would appear to be correlated with the phyllosilicate fraction subtype of the CM chondrites (Howard et al. 2015) (*i.e.*, CM1.6 Y-791198 > CM1.4 LEW 90500 > CM1.3 LON 94101 > CM1.2 ALH 83100, except for A-881458 that was not investigated in Howard et al. (2015)).

For the CR chondrites, total HAA content in each extract ranged from 0.42 ± 0.01 nmol/g for the HW extract of GRO 95577 (CR1, CR2.0/1.3/1.3) to 171 ± 1 nmol/g for the HW extract of MIL 07525 (CR2, CR2.8) (**Table 1-3**). The trend of combined HAA abundances in the two extracts (HW + HCl extracts) of CR chondrites followed the order of MIL 07525 (CR2, CR2.8), 315 ± 6 nmol/g > MET 00426 (CR2, CR2.8/2.6/2.6), 274 ± 13 nmol/g > LAP 02342 (CR2, CR2.8/2.7/2.5), 204 ± 10 nmol/g > GRO 95577 (CR1, CR2.0/1.3/1.3), 10 ± 1 nmol/g, which is generally correlated with the subtype based on the degree of hydration (wt% H in water and OH) of the CR carbonaceous chondrites (Alexander et al. 2013) (*i.e.*, CR2.6 MET 00426 > CR 2.5 LAP 02342 > CR1.3 GRO 95577, except for MIL 07525 that was not investigated by Alexander et al. (2013)).

Interestingly the CR2 chondrites (MIL 07525, LAP 02342, and MET 00426) contained greater abundances of the individual HAAs, serine and α -methylserine when

summed from their respective HW + HCl extracts, than any other α -HAA detected in the summed HW + HCl extracts of any of the CM and CR meteorites (**Table 1-4**). The total abundances of α -HAAs were higher in the CR2 chondrites compared to the CM2 chondrites. In contrast to this disparity among α -HAAs, the abundances of β - and γ -HAAs in CR chondrites were within a similar range to those in CM chondrites. For example, the combined β -HAA abundances in the two extracts of each CR chondrite ranged from 0.82 ± 0.01 nmol/g for GRO 95577 to 18 ± 1 nmol/g for MIL 07525, while those of CM chondrites ranged from 0.69 ± 0.02 nmol/g for ALH 83100 to 37 ± 1 nmol/g for Y-791198. Likewise, the combined γ -HAA abundances in the two extracts of each CR chondrite ranged from 0.112 ± 0.005 nmol/g for GRO 95577 to 1.3 ± 0.1 nmol/g for MIL 07525), while those of CM chondrites ranged from 0.098 ± 0.002 nmol/g for ALH 83100 to 3.14 ± 0.09 nmol/g for Y-791198. This trend marks the first reporting of disparities between total abundances of α -HAAs compared to β - and γ -HAAs in CM and CR chondrites, possibly indicating that varying formation pathways may be responsible for the observed differences.

It is also worth noting that, for all CR2 meteorites and most of the CMs studied here, the HCl extracts are the only ones that contain γ -HAAs. Exposure of γ -HAA precursors in the meteorite matrix to HCl during the extraction process might induce the formation or liberation of γ -HAAs, or their precursors to allow synthesis during workup. Further work is needed to investigate whether a discrepancy among structural amino acid isomer distributions between HW and HCl extracts would also be observed for conventional amino acids (*e.g.*, C₅ amino acid isomers, as investigated in previous works (Elsila et al. 2016 and references therein)).

Fig. 1-5A and Fig. 1-5B show the relative abundances of C₃ and C₄ HAAs in the HW and HCl extracts, respectively, as a function of amine position (α -, β -, or γ -) relative to the total abundance of C₃ and C₄ HAAs. The relative abundances were calculated from the data in **Table 1-2** and **Table 1-3**. The relative abundances of α -HAAs were larger than those of β -HAAs and γ -HAAs, for the HW and HCl extracts of all CM and CR chondrites (**Fig. 1-5A and**

Fig. 1-5B). It must be noted that the relative abundances in the HCl extract of GRO 95577 were biased toward α -HAA isomers by relatively significant L-serine and L-threonine abundances that were likely due to terrestrial contamination (see **Table 1-2** and **Table 1-3**). The relative abundances of β -HAAs in HCl extracts were comparable to, or greater than, those in HW extracts for all meteorites except LON 94101 and GRO 95577. Similarly, the relative abundances of γ -HAAs in HCl extracts were comparable to, or greater than, those in HW extracts for all meteorites except GRO 95577. The stark contrast in relative abundances between the HW extract of CR1 GRO 95577 and all the other extracts of all the other CRs studied here is intriguing. Further work is needed to determine the genesis of this difference, but that is beyond the scope of the present study.

Fig. 1-5C shows the relative HAA abundances in the combined (HW + HCl) extracts of CM and CR chondrites, as a function of amine position (α -, β -, or γ -). The α -HAA isomers dominate the distribution of C₃ and C₄ HAA isomers for all meteorites. In particular, the CR2 chondrites (MIL 07525, LAP 02342, and MET 00426) showed much larger relative abundances of α -HAA isomers than β - or γ -HAA isomers, which were derived from abundant serine and α -methylserine (see **Table 1-3**). In contrast, the CM2 chondrites (Y-791198, A-881458, LEW 90500, and LON 94101) possessed noticeably greater relative abundances of β - and γ -HAAs than the CR chondrites studied here. The disparities between the relative abundances of α -HAAs, and β - and γ -HAAs in the CM2 and CR2 chondrites might indicate that different HAA formation mechanisms had occurred in CM and CR chondrite parent bodies.

1.3.3. Enantiomeric Compositions of Non-Proteinogenic Hydroxy Amino Acids

Since α -dialkyl amino acids, such as isovaline, have been targeted in previous meteorite studies to evaluate their enantiomeric excesses in meteorites, given their resistances to racemization (Pollock et al. 1975), a similar α -dialkyl HAA, α -methylserine, was targeted in this study to explore its possible enantiomeric excess in meteorites. We first resolved D,L-

α -methylserine in carbonaceous chondrites using the developed GC-MS method (**Fig. 1-3 and Fig. 1-4**). However, it was found that α -methylserine was racemic within error in most carbonaceous chondrite extracts (**Table 1-5**). Thus, the α -methylserine in CM and CR chondrites did not appear to show convincing L-enantiomeric excesses correlating with the degree of aqueous alteration, a phenomenon observed in the α -dialkyl amino acid, isovaline (Elsila et al. 2016 and references therein; Glavin et al. 2020a,b).

The notable exceptions to this observation of racemic α -methylserine included the HCl extracts of LEW 90500 and MET 00426, and the HW extracts of LON 094101 and MIL 07525. These extracts of LEW 90500 and LON 094101 contained very nearly racemic mixtures of α -methylserine that were slightly L-enantiomerically enriched, outside of the measurement error, as they exhibited α -methylserine D/L ratios of 0.95 ± 0.02 and 0.96 ± 0.01 , respectively (**Table 1-5**). The aforementioned extracts of MIL 07525 and MET 00426 showed slight D- α -methylserine enantiomeric enrichments outside of errors, as they exhibited α -methylserine D/L ratios of 1.11 ± 0.02 and 1.14 ± 0.02 , respectively (**Table 1-5**). These narrow L- or D- α -methylserine enantiomeric excesses observed outside of errors are anomalous compared to the α -methylserine data collected from most other meteorite extracts analyzed here. They are also inconsistent with the findings from their respective HW or HCl extract counterparts for the same samples, which showed α -methylserine was racemic. Future quantitative analyses are necessary to determine if these anomalies are similarly observed by alternative analytical methodologies, such as ultraperformance liquid chromatography with fluorescence detection and time-of-flight mass spectrometry (UPLC-FD/ToF-MS) (Glavin et al., 2020b).

The other non-proteinogenic α -HAAs, namely *allo*-threonine and homoserine, in most carbonaceous chondrites were affected by coelution with interfering species, which made accurate quantification of their enantiomers not possible (**Fig. 1-3 and Fig. 1-4**). Some meteorite extracts showed the chromatographic peaks of *allo*-threonine and homoserine without coelution. In these cases, *allo*-threonine and homoserine were racemic within

analytical errors, except for homoserine in ALH 83100 (**Table 1-5**). The L-enantiomeric excess for homoserine observed in the HW and HCl extracts of ALH 83100 were $51.7 \pm 1.2\%$ and $8.0 \pm 1.6\%$, respectively (**Table 1-5**). However, it should be noted that L-homoserine can be produced by methionine metabolism as a terrestrial biological component (Matsuo and Greenberg 1955). Furthermore, in this study, we observed significantly abundant L-serine and L-threonine in both extracts of ALH 83100, which were considered to be terrestrial contamination (**Table 1-2**). Thus, it is plausible that the L-enantiomeric excesses of homoserine in the HW and HCl extracts of ALH 83100 could also be derived from terrestrial contamination.

1.3.4. A Proposed Formation Mechanism for Prominent α -Hydroxy Amino Acids: Strecker-Cyanohydrin Synthesis

This study revealed that α -methylserine and serine were significantly more abundant in the combined (HW + HCl) extracts of CR2 chondrites (LAP 02342, MET 00426, and MIL 07525) than other α -HAAs, such as threonine, *allo*-threonine, and homoserine (**Table 1-4**). These abundances of serine and α -methylserine may be explained by the predominance of the Strecker-cyanohydrin synthesis within the parent bodies of the CR chondrites, as has been proposed for the abundances of other α -amino acids in meteorite samples (Peltzer and Bada, 1978; Peltzer et al., 1984; Lerner et al., 1993; Glavin et al. 2010). The predominance of α -methylserine and serine compared to other α -HAAs could be used to make inferences about the relative abundances of α -HAA precursors in CR chondrite parent bodies. The carbonyl precursor of α -methylserine and serine is hydroxyacetone and glycolaldehyde, respectively, and threonine and/or *allo*-threonine and homoserine would be from lactaldehyde and 3-hydroxypropanal, respectively, as illustrated in the proposed formation mechanisms shown in **Fig. 1-6**.

One potential explanation for the observed abundance disparities between more prevalent α -HAAs (serine and α -methylserine) and less prevalent α -HAAs (threonine, *allo*-threonine, and homoserine) is by the different production quantities of necessary carbonyl

precursors via radical chemistry in the interstellar environments (**Fig. 1-7**). Precursor carbonyl compounds in carbonaceous chondrites could have originated from interstellar environments before incorporation into meteorite parent bodies, as indicated by the heavy carbon and hydrogen isotopic compositions of resultant α -amino acids (Elsila et al. 2012; Pizzarello and Huang 2005; Pizzarello et al. 2004). To illustrate, the irradiation of CH₃OH-rich ices on the grain surface can generate CH₃CO, HCO, and CH₂OH radicals (Öberg et al. 2009) (**Fig. 1-7**). The radicals' recombination can yield hydroxyacetone and glycolaldehyde, which are precursors of α -methylserine and serine, respectively. Similarly, the radicals CH₃CHOH and CH₂CH₂OH can be derived from ethanol (C₂H₅OH), which is less abundant than methanol in the interstellar medium (Bisschop et al. 2008), and can recombine to form aldehyde precursors of threonine, *allo*-threonine, and homoserine (*i.e.*, lactaldehyde and 3-hydroxypropanal). Hence, the observed abundance disparities between more abundant α -HAAs and less abundant α -HAAs might be derived from more abundant methanol than ethanol in the interstellar ices. The potential role of radical chemistry to facilitate precursor carbonyl synthesis before the Strecker synthesis of α -HAAs, warrants further investigation.

A critical aspect of the Strecker cyanohydrin synthesis that could have contributed to elevated abundances of α -methylserine and serine in the extracts of the CR2 chondrites studied here is the abundance of ammonia on the meteorite parent bodies. To explain, Pizzarello et al. (2011) reported that CR2 chondrites were more enriched in ammonia than CM2 chondrites, and that ammonia was present not only in the free form but also in a bound form that can be released from insoluble organic matter by hydrothermal treatment. Meteoritic parent bodies with reducing environments, similar to those of CR2 chondrite parent bodies, could have possessed more ammonia. In turn, the Strecker cyanohydrin synthesis (see **Fig. 1-6** for examples) could have proceeded on such parent bodies by forming an imine from ammonia and a precursor aldehyde or ketone. The imine could then react with HCN to form an aminonitrile that becomes hydrolyzed to yield an α -amino acid (Peltzer and Bada, 1978; Peltzer

et al., 1984). However, in more oxidized, ammonia-depleted environments, similar to those of CM2 chondrite parent bodies), the Strecker cyanohydrin synthesis would be more likely to proceed by forming a cyanohydrin, as opposed to an aminonitrile, where the cyanohydrin could subsequently be hydrolyzed to yield an α -hydroxy acid (Peltzer and Bada, 1978; Peltzer et al., 1984). In this work, the CM2 chondrites (Y-791198, A-881458, LEW 90500, and LON 94101) were found to contain smaller relative abundances of α -HAAs than the CR2 chondrites (MIL 07525, LAP 02342, and MET 00426) (**Fig. 1-5C**). One potential explanation for this observation could be differences in the ammonia concentrations in the CR and CM chondrite parent bodies.

Such a difference of ammonia concentrations between CM and CR chondrites could infer the different redox conditions of their parent bodies, which have been exhibited by their elemental distributions, mineralogies, and N-heterocyclic compounds distribution. For instance, X-ray absorption near edge structure spectroscopy showed that CM chondrites contained more oxidized carbon and organic sulfur than CR chondrites (Le Guillou et al. 2014; Orthous-Daunay et al. 2010). Mineralogical observations have revealed that CM chondrites contain more abundant oxides and sulfides in the matrix than CR chondrites (*i.e.*, iron exists as +2 (and +3) valent Fe), while CR chondrites possess more abundant metals (*i.e.*, iron exists as zero-valent Fe) (Howard et al. 2015; Naraoka and Hashiguchi 2019). Naraoka and Hashiguchi (2019) suggested that although N-heterocyclic compounds in CM chondrites were synthesized as alkyipyridines ($C_nH_{2n-5}N$) under more oxidizing conditions, the compounds in CR chondrites were produced as alkyipiperidines ($C_nH_{2n+1}N$) under more reducing conditions. Therefore, all of these lines of evidence support that the difference in the reducing or oxidizing natures of CM and CR chondrite parent bodies may be at least partially responsible for the observed disparities in α -HAA relative abundances between the CM2 and CR2 chondrites that were focused on in this work.

1.3.5. A Proposed Formation Mechanism for β -, and γ -Hydroxy Amino Acids: Ammonia-Involved Formose-like Reaction

Previous reports suggest that the Strecker cyanohydrin synthesis can form α -amino acids, but not β - and γ -amino acids (Elsila et al. 2012 and references therein). Consequently, to explain the distribution of HAA structural isomers observed in the carbonaceous chondrites studied here, a complementary formation mechanism is required. The syntheses of β - and γ -HAAs were observed in laboratory experiments performed by Koga and Naraoka (2017), which produced 17 amino acids, including α -, β -, and γ -HAAs, from formaldehyde, acetaldehyde, glycolaldehyde, and ammonia in aqueous solution at 60 °C for 6 days. Insight into how structural diversity of HAAs may have been formed in the parent bodies of the meteorites focused on in this study may be gleaned from a combination of the formose reaction and the experiments outlined in Koga and Naraoka (2017). In the formose reaction, glycolaldehyde, and eventually sugars, are formed from the condensation of formaldehyde molecules in alkaline solution (Breslow 1959). It has been proposed that the formation of β - and γ -HAAs may follow a similar line of synthesis, whereby aldehydes (*e.g.*, formaldehyde and glycolaldehyde) in the presence of ammonia, could yield amino acids via the formose reaction and aldol condensation (Koga and Naraoka 2017). The nomenclature for such a formation pathway for β - and γ -HAAs could be considered the ammonia-involved formose-like reaction. A similar reaction has been recognized to produce chondritic insoluble organic matter-like organic solids (Kebukawa et al. 2013) and various soluble organic compounds, including N-bearing compounds (Kebukawa et al. 2020) and conventional amino acids other than HAAs (Kebukawa et al. 2017).

The ammonia-involved formose-like reaction is distinct from the Strecker cyanohydrin reaction because the ammonia-involved formose-like reaction does not require HCN to produce amino acids, whereas the Strecker cyanohydrin reaction does. The presence of β - and γ -HAA isomers found in all the carbonaceous chondrites analyzed in this work

indicates that a similar reaction to the ammonia-involved formose-like reaction may have occurred on the parent bodies of the meteorites studied here, which could have complemented the Strecker cyanohydrin synthesis to generate HAA structural diversity. In particular, more predominant relative abundances of β - and γ -HAAs in CM chondrites (**Fig. 1-5C**) may suggest that a synthetic process like the ammonia-involved formose-like reaction could have occurred more prominently in the parent bodies of CM chondrites than CR chondrites.

The abundance differences between α -HAAs and β -HAAs, namely serine and isoserine, respectively, in the less altered CR chondrites may provide insight into the formation mechanisms responsible for their syntheses and the periods in which these syntheses could have occurred on the meteorite parent bodies. Pizzarello et al. (2008, 2010, 2012) proposed that much of the amino acid syntheses could have occurred early in the parent body's history based on the abundances of short-chain amino acids (*e.g.*, glycine and alanine) in CR2 chondrites. Extrapolation of this hypothesis to the less altered CR chondrites analyzed in this study suggests that 1) the Strecker cyanohydrin synthesis might have predominated early and 2) the ammonia-involved formose-like reaction could have occurred later in their parent body histories to produce the observed serine and isoserine abundances. For the Strecker cyanohydrin synthesis to have predominated early, the parent body environment would have needed to be ammonia- and HCN-rich to facilitate the formation of α -amino acids, including serine (**Fig. 1-6**). Over time, HCN abundances on the parent bodies could have become depleted due to consumption via the Strecker-cyanohydrin reaction, HCN polymerization (Lerner et al. 1993), and/or metal-cyanide complexation (Smith et al. 2019). Such HCN-poor environments may not have boded well for the viability of the Strecker cyanohydrin synthesis to produce α -amino acids. However, the ammonia-involved formose-like reaction occurs readily in cyanide-depleted scenarios to produce a mixture of both α - and β -amino acids, namely α -HAA serine and β -HAA isoserine, from aldehydes and ammonia (Koga and Naraoka, 2017). Therefore, the depletion of HCN on the meteorite parent bodies could have marked the

transition from serine production dominated by the Strecker cyanohydrin synthesis to the formation of both serine and isoserine dominated by the ammonia-involved formose-like reaction.

1.4. Conclusion

The research presented here entailed the analyses of five CM chondrites and four CR chondrites to examine the abundances, distributions, and enantiomeric ratios of a suite of HAAs in the HW and 6 M HCl extracts of these chondrites. To perform the necessary HAA analyses, we developed a new GC-MS analytical technique to target 13 HAAs, including α -, β -, and γ -HAAs.

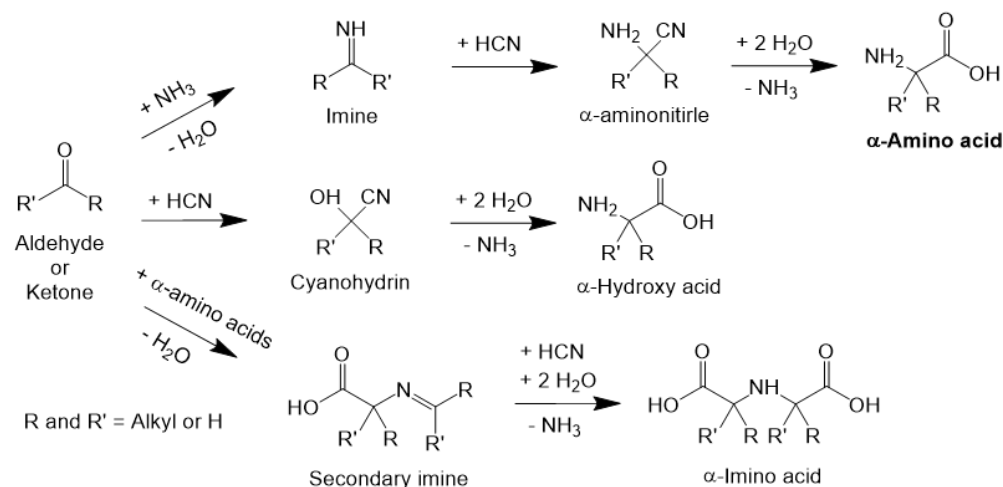
The HAA analyses performed in this study revealed that distinct differences in α -HAA distributions existed between CR and CM chondrites, which are groups of chondrites with different chemistries. Elevated abundances of the α -hydroxy amino acids serine and α -methylserine were observed more prominently in the CR2 chondrites than the CM chondrites. In contrast to α -HAAs, total abundances of β - and γ -HAAs were similar between the CM and CR chondrites. The total HAA abundances of the CM and CR chondrites generally appeared to be inversely proportional to the degree of aqueous alteration in the parent bodies, as determined by the phyllosilicate fraction (Howard et al., 2015) for CM chondrites and the degree of hydration (Alexander et al. 2013) for CR chondrites, respectively. However, A-881458 and MIL 07525 are not necessarily included in this assessment as these two chondrites are not currently classified based on these criteria. Furthermore, ALH 83100 is also not included in this assessment due to the likely significant L-serine and L-threonine contamination observed, skewing the total HAA abundance observed for this meteorite. A plurality of non-proteinogenic HAAs, including α -methylserine, did not show enantiomeric excesses correlating with the degree of the aqueous alteration, a phenomenon observed in meteoritic isovaline (Glavin and Dworkin, 2009). Further investigations are needed to verify enantiomeric excesses of α -methylserine and homoserine in select carbonaceous chondrite extracts with quantitative analyses using UPLC-FD/ToF-MS and isotopic analyses using gas chromatography-combustion-isotope ratio mass spectrometry.

The elevated total abundances of α -HAAs in CR2 chondrites could be produced by

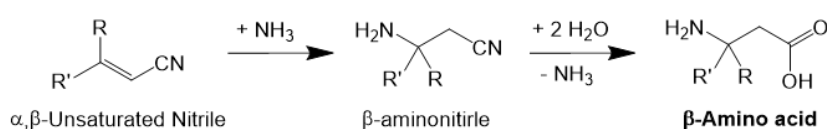
the Strecker cyanohydrin reaction, which may dominate under reducing conditions containing abundant ammonia in the meteorite parent body, as suggested by Pizzarello et al. (2011). The radical chemistry of more abundant methanol than ethanol in the interstellar ices might explain the observed abundance disparities between more prevalent α -HAAs (serine and α -methylserine) and less prevalent α -HAAs (threonine, *allo*-threonine, and homoserine). The ubiquitous presence of β - and γ -HAAs in CM and CR chondrites, but more predominantly in the CM chondrites studied here, might infer that a process similar to the ammonia-involved formose-like reaction proceeded in the meteorite parent bodies (Koga and Naraoka 2017), and perhaps more so in the parent bodies of CM chondrites than CR chondrites. Based on the significant differences in abundances between α - and β -HAAs in CR2 chondrites, the ammonia-involved formose-like reaction could have proceeded after the predominance of the Strecker cyanohydrin synthesis in the parent body histories.

1.5. Figures

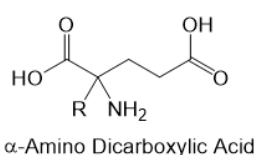
Strecker Cyanohydrin Reaction



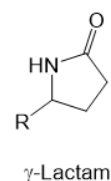
Michael Addition



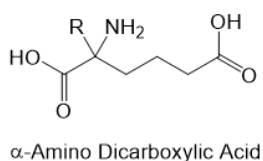
Decarboxylation



Hydrolysis of Lactam



Decarboxylation



Hydrolysis of Lactam

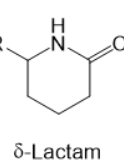


Fig. 1-1. Plausible formation mechanisms for α -, β -, γ -, and δ -amino acids.

α -amino acids can be formed by the Strecker-cyanohydrin pathway. β -amino acids can be formed by Michael addition of ammonia to α, β -unsaturated nitriles. γ - and δ -amino acids can be formed by decarboxylation of α -amino dicarboxylic acids or by the hydrolysis of lactams found in meteorites. Detailed explanations for each chemical formation pathway are described in the text. This figure is slightly modified from FIGURE 3.7 in Glavin et al. 2018.

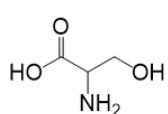
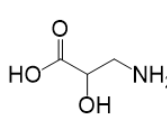
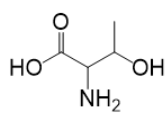
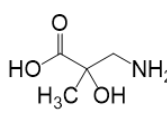
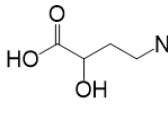
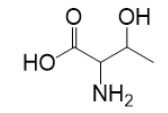
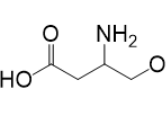
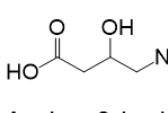
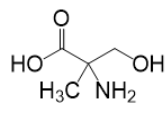
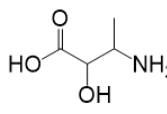
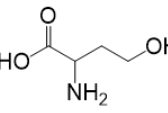
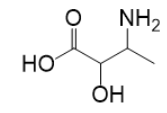
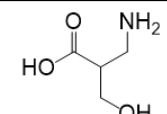
α -amino	β -amino	γ -amino
C_3	C_3	
 Serine	 Isoserine*	
C_4	C_4	C_4
 Threonine	 α -Methylisoserine**	 4-Amino-2-hydroxybutanoic acid*
 <i>allo</i> -Threonine	 β -Homoserine*	 4-Amino-3-hydroxybutanoic acid*
 α -Methylserine*	 Isothreonine*	
 Homoserine*	 <i>allo</i> -Isothreonine*	
	 3-Amino-2-(hydroxymethyl)propanoic acid*	

Fig. 1-2. All the structural isomers of C_3 and C_4 hydroxy amino acids investigated in this study.

* Hydroxy amino acids identified in the Murchison (CM2) meteorite by Koga and Naraoka (2017).

** Although a peak whose mass spectrum corresponding to the structure of α -methylisoserine was detected in the Murchison meteorite by Koga and Naraoka (2017), proper identification of the peak was not possible in that reporting due to the unavailability of the necessary analytical standard.

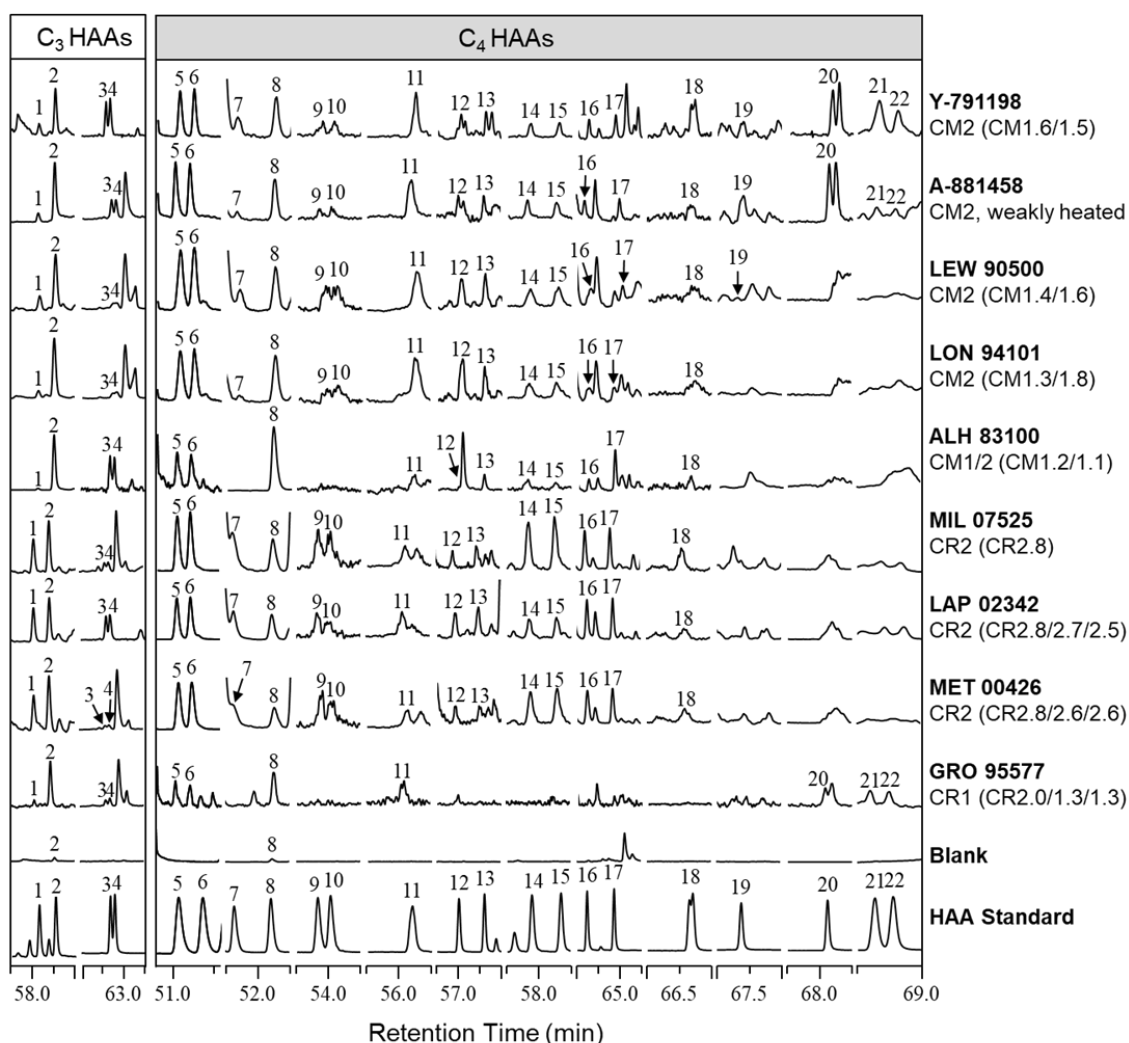


Fig. 1-3. The selected regions of the GC-MS extracted ion chromatograms of the C₃ and C₄ hydroxy amino acids in the HW extracts of the CM and CR chondrites studied here.

Peak identifications are as follows: 57.5–59.0 min for 1) D-serine and 2) L-serine; 62.0–63.5 min for 3) D-isoserine and 4) L-isoserine; 50.6–51.6 min for 5) L- α -methylserine and 6) D- α -methylserine; 51.5–52.5 min for 7) D-threonine and 8) L-threonine; 53.5–54.5 min for 9) D- or L-isothreonine and 10) D- or L-isothreonine; 55.5–56.5 min for 11) DL- α -methylisoserine; 56.5–58.0 min for 12) D-*allo*-threonine and 13) L-*allo*-threonine; 57.5–58.5 min for 14) D- or L-*allo*-isothreonine and 15) D- or L-*allo*-isothreonine; 64.0–65.5 min for 16) D-homoserine and 17) L-homoserine; 66.0–67.0 min for 18) DL- β -homoserine; 67.0–68.0 min for 19) D-3-A-2-HMPA; 67.5–68.5 min for 20) L-4-A-2-HBA; and 68.5–69.0 min for 21) D-4-A-3-HBA and 22) L-4-A-3-HBA. The fragment ions used to generate each chromatogram shown here are detailed in **Table S1**.

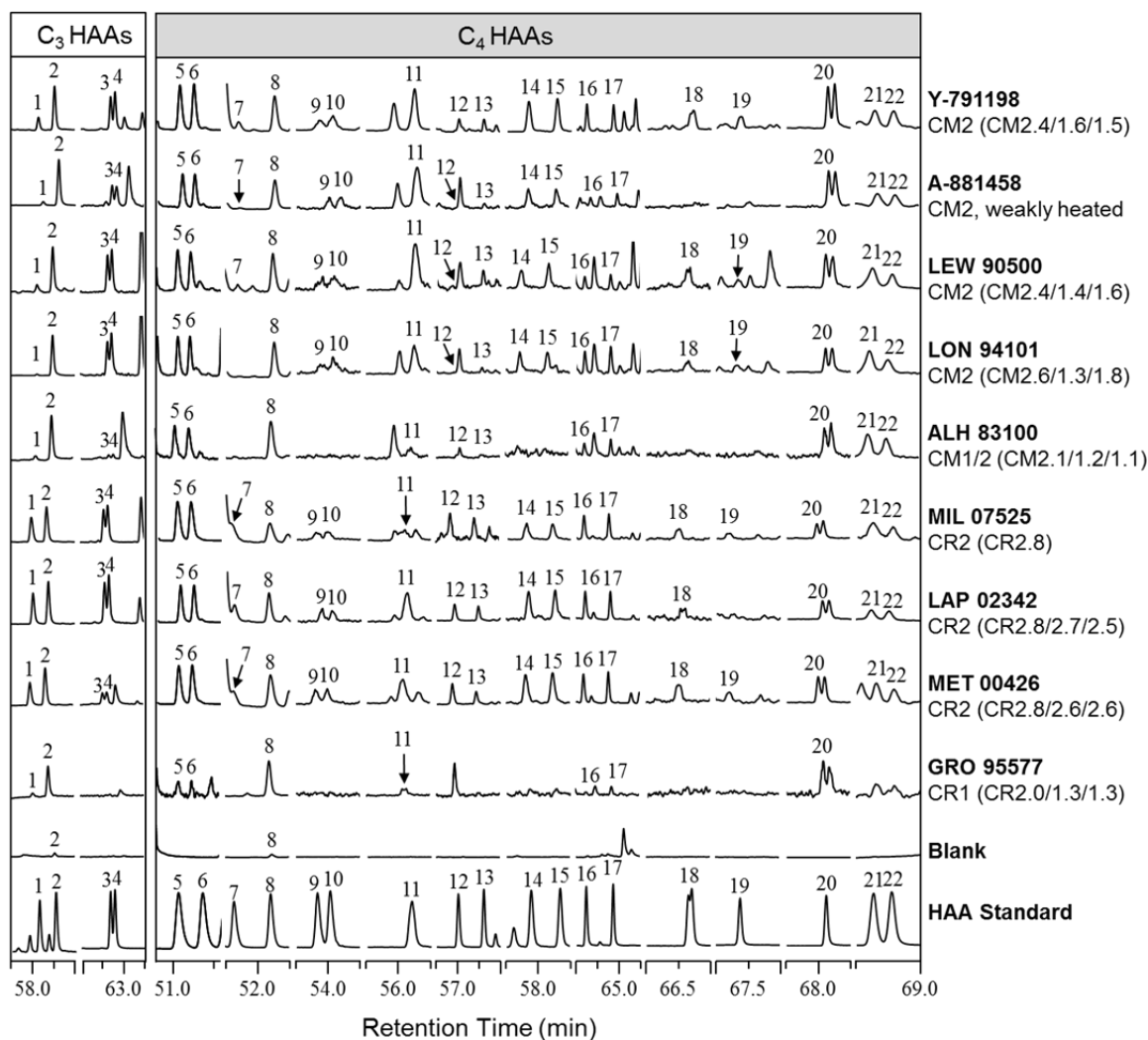


Fig. 1-4. The selected regions of the GC-MS extracted ion chromatograms of the C₃ and C₄ hydroxy amino acids in the 6 M HCl extracts of the CM and CR chondrites studied here. Peak identifications are the same as in Fig. 2. The fragment ions used to generate each chromatogram shown here are detailed in **Table S1**.

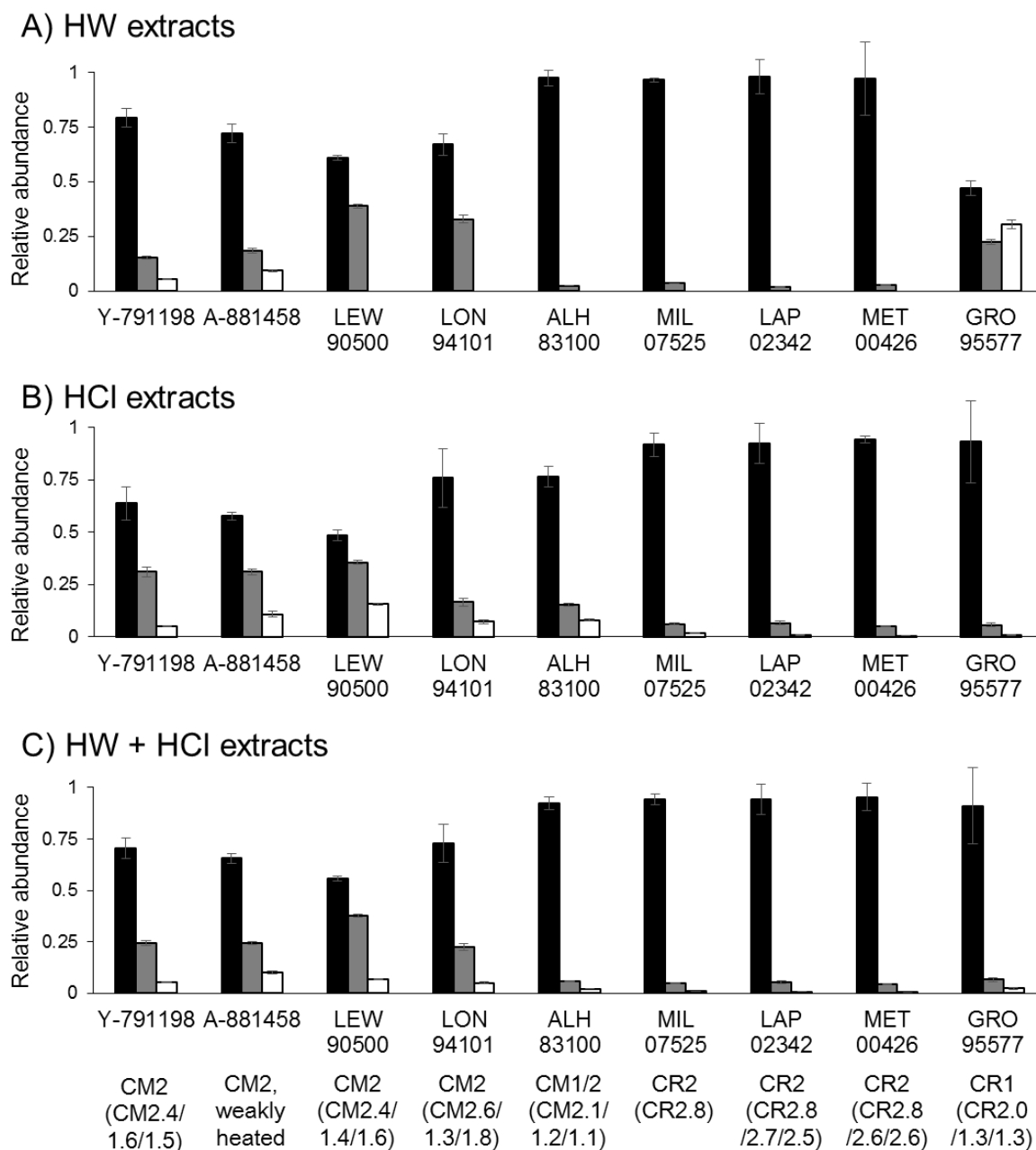


Fig. 1-5. The relative abundances of C₃ and C₄ hydroxy amino acids in CM and CR carbonaceous chondrites for A) the HW extracts, B) the HCl extracts, and C) the combined (HW + HCl) extracts.

Relative abundances are displayed as functions of amine position (α -, β -, γ -) relative to the total abundance of C₃ and C₄ hydroxy amino acids. The relative abundances were calculated from the data in **Table 1-2** and **Table 1-3**, and the uncertainties were determined by appropriate propagation of the standard errors. In all figure panes, black bars denote α -amines, grey bars denote β -amines, and white bars denote γ -amines.

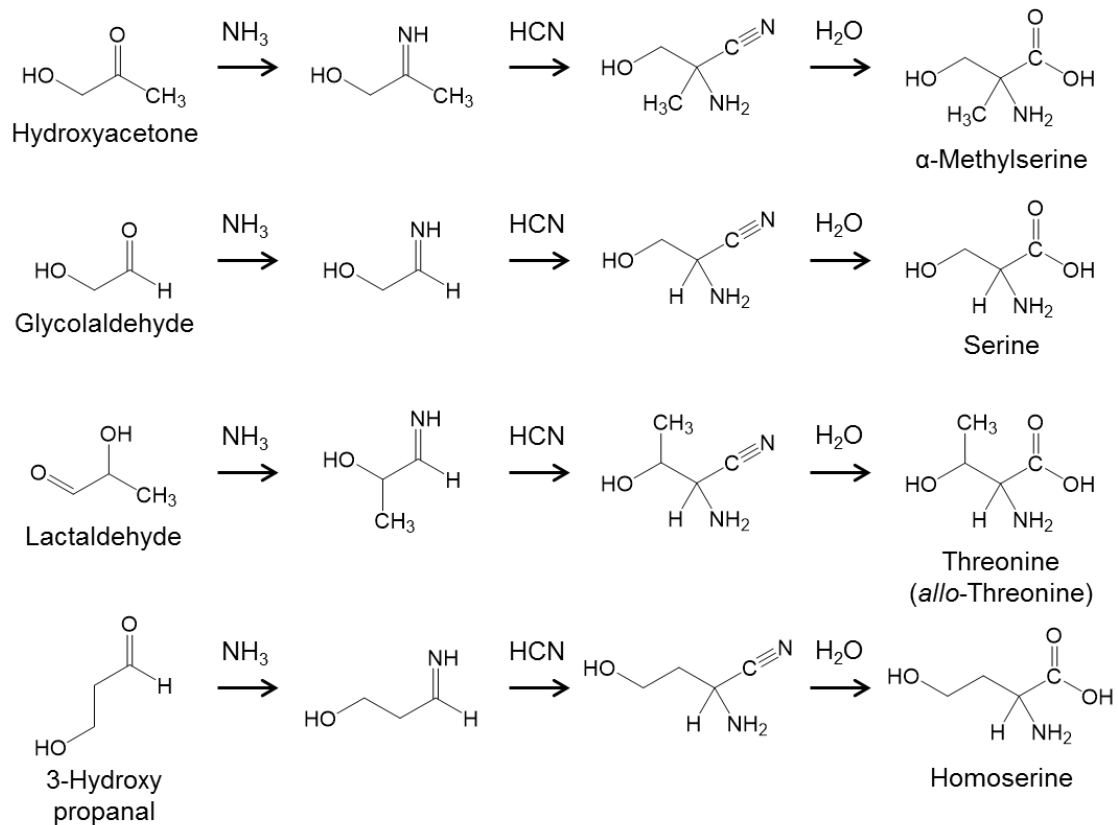


Fig. 1-6. Examples of the proposed synthetic pathways for the formation of select α -hydroxy amino acids via the Strecker cyanohydrin reaction.

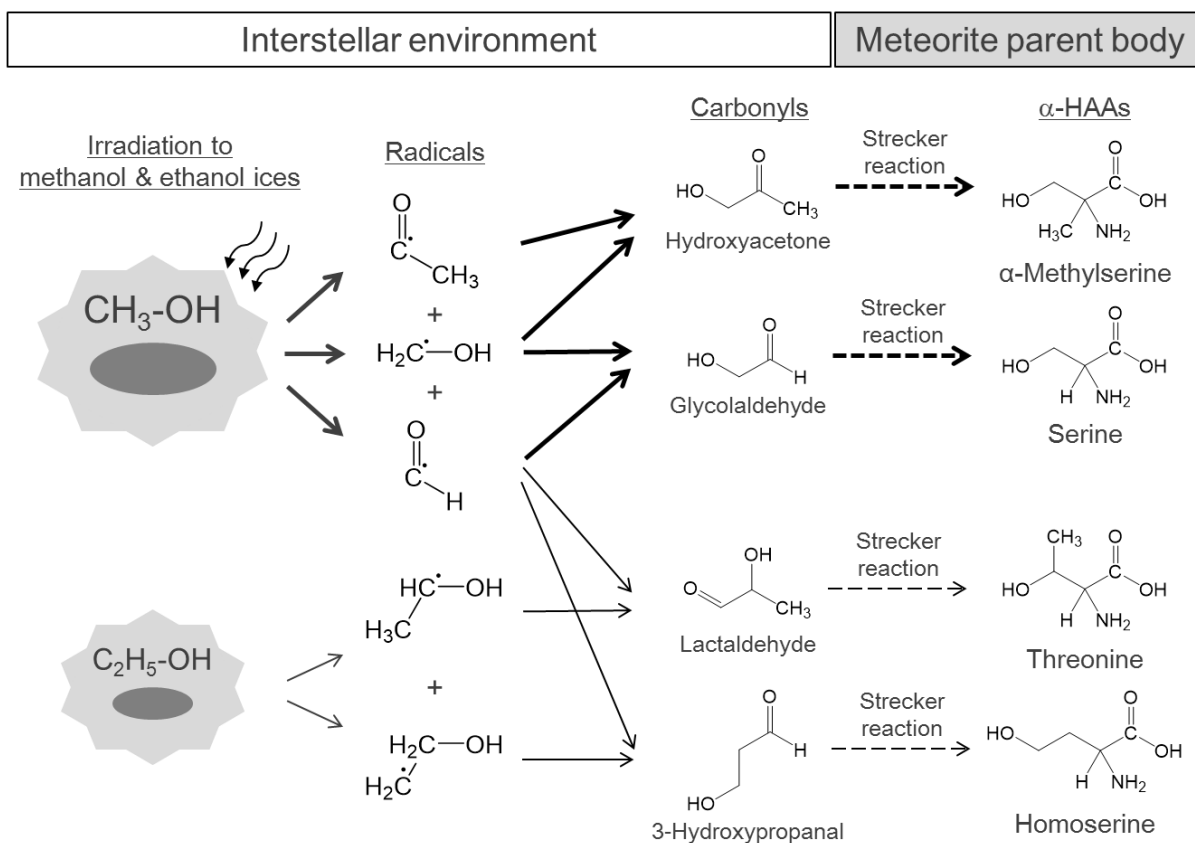


Fig. 1-7. The recombination of select free radical pairs to form carbonyl compounds, which serve as precursors for forming C₃ and C₄ α -hydroxy amino acids.

1.6. Tables

Table 1-1. Meteorite samples analyzed in this study.

Meteorite ^a	Petrographic Type	Subtype (petrology)	Subtype (phyllosilicate fraction) ^b	Subtype (H in OH/H ₂ O) ^c	Mass extracted (mg)	Fragment (specific, parent)
Y-791198	CM2	2.4 ^d	1.6	1.5	138.9	
A-881458	CM2, very weakly heated ^e	–	–	–	176.4	
LEW 90500	CM2	2.4 ^f	1.4	1.6	364.4	89, 2
LON 94101	CM2	2.6 ^f	1.3	1.8	274.0	101, 8
ALH 83100	CM1/2	2.1 ^f	1.2	1.1	280.4	302, 279
MIL 07525	CR2 ^g	2.8 ^h	–	–	273.1	17, 0
LAP 02342	CR2	2.8 ^h	2.7	2.5	298.1	64, 0
MET 00426	CR2	2.8 ^h	2.6	2.6	327.3	78, 0
GRO 95577	CR1	2.0 ^h	1.3	1.3	342.1	9, 0

^a Abbreviations: Asuka, A-; Yamato, Y-; Lewis Cliffs, LEW; Lonewolf Nunataks, LON; Allan Hills, ALH; Miller Range, MIL; Meteorite Hills, MET; La Paz Icefield, LAP; Grosvenor Mountains, GRO.

^b After Howard et al. (2015).

^c After Alexander et al. (2013).

^d After Rubin et al. (2007)

^e After Nakamura (2005) and Kimura et al. (2011).

^f Estimated using correlations between petrologic type and bulk H and N isotopes from Alexander et al. (2013).

^g Although Antarctic Meteorite Newsletter, 34 and NASA Antarctic Meteorite Petrographic Description (<https://curator.jsc.nasa.gov/antmet/samples/petdes.cfm?sample=MIL07525>, accessed on 2/24/2021) classified MIL 07525 as a CR3, subsequent reporting (*e.g.*, Vollmer et al. 2020) has regarded MIL 07525 as a CR2 because of abundant secondary phases.

^h After Harju et al. (2014).

Table 1-2. Summary of the average abundances (nmol/g) of the three- to four-carbon hydroxy amino acids identified in the HW and HCl extracts of CM carbonaceous chondrites measured by GC-MS^a.

Hydroxy amino acids (Amine position)	Y-791198		A-881458		LEW 90500		LON 94101		ALH 83100	
	CM2 (CM2.4/1.6/1.5)		CM2, very weakly heated		CM2 (CM2.4/1.4/1.6)		CM2 (CM2.6/1.3/1.8)		CM1/2 (CM2.1/1.2/1.1)	
	Hot water	HCl	Hot water	HCl	Hot water	HCl	Hot water	HCl	Hot water	HCl
D-Serine (α)	4.2 ^b	7 ± 2	0.29 ± 0.01	0.67 ± 0.03	0.088 ± 0.007	0.137 ± 0.005	0.12 ± 0.02	0.26 ± 0.05	0.16 ± 0.01	0.14 ± 0.01
L-Serine (α)	9.5 ^b	18 ± 4	2.2 ± 0.2	1.60 ± 0.07	0.24 ± 0.03	0.69 ± 0.07	0.7 ± 0.1	2.1 ± 0.5	5.0 ± 0.2	1.05 ± 0.09
DL-Isoserine ^c (β)	1.40 ± 0.03	8.2 ± 0.4	0.53 ± 0.02	0.46 ± 0.03	0.44 ± 0.02	0.149 ± 0.006	0.369 ± 0.008	0.125 ± 0.009	0.133 ± 0.004	0.41 ± 0.01
L- α -Methylserine (α)	12 ± 1	7.8 ± 0.5	1.13 ± 0.07	0.366 ± 0.009	0.749 ± 0.009	0.133 ± 0.001	0.272 ± 0.003	0.20 ± 0.03	0.034 ± 0.002	0.126 ± 0.004
D- α -Methylserine (α)	13 ± 1	7.9 ± 0.5	1.2 ± 0.1	0.38 ± 0.01	0.76 ± 0.01	0.127 ± 0.002	0.261 ± 0.001	0.19 ± 0.02	0.0347 ± 0.0005	0.120 ± 0.006
D-Threonine (α)	0.40 ± 0.07	0.35 ± 0.05	0.033 ± 0.004	0.019 ± 0.007	0.061 ± 0.002	0.0140 ± 0.0002	0.013 ± 0.001	0.013 ± 0.001	n.d.	n.d.
L-Threonine (α)	0.6 ± 0.1	1.2 ± 0.2	0.22 ± 0.01	0.75 ± 0.04	0.106 ± 0.004	0.077 ± 0.002	0.124 ± 0.003	0.41 ± 0.05	1.66 ± 0.06	0.35 ± 0.01
D- <i>allo</i> -Threonine (α)	0.14 ^d ± 0.02	0.22 ± 0.02	0.034 ^d ± 0.003	0.017 ^d	0.059 ^d ± 0.003	0.012 ^d	0.018 ^d	0.017 ^d	0.054 ^d	0.013 ^d
L- <i>allo</i> -Threonine (α)	0.19 ^d ± 0.04	0.22 ± 0.02	0.036 ^d ± 0.003	0.017 ± 0.003	0.050 ± 0.004	0.012 ± 0.001	0.018 ± 0.002	0.017 ^d ± 0.001	0.054 ± 0.004	0.013 ± 0.001
D-Homoserine (α)	0.62 ^d ± 0.07	0.99 ^d ± 0.04	0.35 ± 0.02	0.063 ± 0.006	0.084 ^d	0.079 ± 0.005	0.040 ^d ± 0.002	0.067 ± 0.009	0.033 ± 0.001	0.0249 ± 0.0005
L-Homoserine (α)	0.61 ± 0.07	0.97 ± 0.04	0.37 ± 0.01	0.084 ^d ± 0.001	0.084 ^d ± 0.005	0.079 ± 0.003	0.038 ^d ± 0.001	0.08 ± 0.01	0.105 ± 0.002	0.0293 ± 0.0008
DL- α -Methylisoserine ^e (β)	5.4 ± 0.2	14.6 ± 0.8	0.86 ± 0.07	1.91 ± 0.09	0.97 ± 0.02	0.85 ± 0.01	0.33 ± 0.02	0.57 ^d ± 0.02	0.045 ± 0.006	0.060 ± 0.006
DL-Isothreonine ^f (β)	0.6 ± 0.1	1.8 ± 0.2	0.18 ± 0.03	0.119 ± 0.006	0.23 ± 0.01	0.087 ± 0.007	0.09 ± 0.02	0.08 ± 0.01	n.d.	n.d.
DL- <i>allo</i> -Isothreonine ^f (β)	0.50 ± 0.03	1.11 ± 0.04	0.095 ± 0.007	0.089 ± 0.006	0.122 ± 0.006	0.048 ± 0.001	0.086 ± 0.006	0.041 ± 0.005	0.019 ± 0.002	n.d.
DL- β -Homoserine ^e (β)	0.98 ± 0.04	0.72 ± 0.03	0.073 ± 0.007	n.d.	0.064 ± 0.002	0.079 ± 0.004	0.08 ± 0.01	0.074 ± 0.002	0.025 ± 0.002	n.d.
D-3-A-2-HMPA ^g (β)	1.0 ^d ± 0.1	0.7 ± 0.1	0.131 ^d ± 0.008	0.11 ± 0.02	n.d.	0.027 ^d ± 0.002	n.d.	0.034 ^d ± 0.002	n.d.	n.d.
L-4-A-2-HBA ^g (γ)	0.78 ^d ± 0.04	1.52 ± 0.08	0.28 ± 0.01	0.24 ± 0.04	n.d.	0.093 ± 0.003	n.d.	0.072 ± 0.008	n.d.	0.038 ± 0.001
D-4-A-3-HBA (γ)	0.352 ^d ± 0.002	0.121 ± 0.005	0.056 ^d ± 0.006	0.08 ^d ± 0.01	n.d.	0.084 ^d ± 0.001	n.d.	0.062 ^d ± 0.003	n.d.	0.036 ^d ± 0.002
L-4-A-3-HBA (γ)	0.23 ± 0.01	0.132 ± 0.007	0.042 ± 0.005	0.06 ± 0.01	n.d.	0.044 ± 0.002	n.d.	0.031 ± 0.002	n.d.	0.0243 ± 0.0008
Total (nmol/g)	52 ± 2 ^g	74 ± 5	8.1 ± 0.3	7.0 ± 0.1 ^g	4.12 ± 0.05 ^g	2.8 ± 0.1 ^g	2.5 ± 0.1 ^g	4.5 ± 0.5 ^g	7.4 ± 0.2 ^g	2.43 ± 0.09 ^g
Sum of HW & HCl (nmol/g)	126 ± 5 ^g		15.2 ± 0.3 ^g		6.94 ± 0.09 ^g		7.0 ± 0.5 ^g		9.8 ± 0.2 ^g	
HW / (HW + HCl)	41 %		54 %		59 %		36 %		75 %	

n.d. = value not determined due to trace amino acid abundances.

^a Sample extracts were analyzed by HFBA-isopropyl derivatization and GC-MS. The reported uncertainties (δx) are based on the standard deviation value (σ) of 2-3 separate measurements (n) with a standard error, $\delta x = \sigma x \cdot (n)^{-1/2}$.

^b Minimum abundances are shown without an accompanying standard error because replicate measurements of this analyte were not made.

^c The enantiomers were not resolved by the chromatographic separation applied in this study.

^d The abundances presented here are approximate due to quantitative interferences posed by non-HAA, coeluting species in the meteorite sample.

^e The abundances were reported as the combined quantity estimates of both enantiomers because although the enantiomers were separated, the elution orders of the respective enantiomers were not determined due to a lack of enantiopure standard availability.

^f Precise abundance estimates are not provided due to the lack of enantiopure standards. Instead, upper limit abundances were estimated.

^g Total abundances were determined using individual HAA abundance estimates that were not accompanied by a standard error, which may cause the true uncertainties of the total abundance estimates to be larger than the total uncertainty estimates provided here.

Table 1-3. Summary of the average abundances (nmol/g) of the three- to four-carbon hydroxy amino acids identified in the HW and HCl extracts of CR carbonaceous chondrites measured by GC-MS^a.

Hydroxy amino acids (Amine position)	MIL 07525 CR2 (CR2.8)		LAP 02342 CR2 (CR2.8/2.7/2.5)		MET 00426 CR2 (CR2.8/2.6/2.6)		GRO 95577 CR1 (CR2.0/1.3/1.3)	
	Hot water	HCl	Hot water	HCl	Hot water	HCl	Hot water	HCl
D-Serine (α)	11 ^b	25 ^b	1.9 ± 0.2	51 ± 7	23 ± 8	38 ± 1	0.0166 ± 0.0005	1.3 ± 0.2
L-Serine (α)	12 ^b	27 ^b	2.1 ± 0.2	52 ± 7	23 ± 10	46 ± 1	0.13 ± 0.01	6 ± 1
DL-Isoserine ^c (β)	1.44 ± 0.09	5.5 ± 0.5	0.43 ± 0.03	1.2 ± 0.1	0.98 ± 0.07	3.1 ± 0.1	0.085 ± 0.005	0.075 ± 0.004
L- α -Methylserine (α)	60.9 ± 0.7	34 ± 4	20 ± 2	14 ± 2	24 ± 1	29.5 ± 0.2	0.0154 ± 0.0003	0.051 ± 0.004
D- α -Methylserine (α)	67.9 ± 0.6	38 ± 4	23 ± 2	14 ± 2	26 ± 2	33.6 ± 0.4	0.014 ± 0.001	0.051 ± 0.001
D-Threonine (α)	2.78 ^d ± 0.04	1.4 ^d ± 0.2	1.3 ^d ± 0.1	1.1 ^d ± 0.2	0.047 ^d ± 0.02	1.6 ^d ± 0.1	n.d.	n.d.
L-Threonine (α)	2.68 ± 0.05	1.8 ± 0.2	1.2 ± 0.1	1.4 ^d ± 0.3	0.84 ± 0.06	3.73 ± 0.06	0.040 ± 0.006	1.3 ± 0.3
D- <i>allo</i> -Threonine (α)	1.81 ± 0.05	0.8 ± 0.1	2.1 ^d ± 0.8	0.5 ± 0.1	0.7 ^d ± 0.1	1.22 ± 0.04	n.d.	n.d.
L- <i>allo</i> -Threonine (α)	2.42 ^d ± 0.09	0.7 ± 0.1	2.2 ^d ± 0.8	0.45 ± 0.08	0.80 ^d ± 0.03	1.32 ^d ± 0.04	n.d.	n.d.
D-Homoserine (α)	1.33 ^d ± 0.08	1.5 ^d ± 0.1	0.54 ^d ± 0.03	0.48 ^d ± 0.03	1.46 ^d ± 0.08	1.02 ± 0.04	0.0049 ^d ± 0.0005	0.022 ^d ± 0.002
L-Homoserine (α)	1.16 ± 0.08	1.5 ^d ± 0.1	0.49 ± 0.02	0.45 ± 0.03	1.36 ± 0.09	0.98 ± 0.05	0.0042 ^d ± 0.0003	0.0475 ^d ± 0.0007
DL- α -Methylisoserine ^e (β)	2.8 ± 0.1	1.9 ^d ± 0.2	0.33 ± 0.04	10 ± 2	1.3 ± 0.1	4.0 ± 0.1	0.047 ± 0.003	0.61 ± 0.01
DL-Isothreonine ^f (β)	1.7 ± 0.1	2.1 ± 0.2	0.272 ± 0.002	0.54 ± 0.06	0.68 ± 0.03	2.42 ± 0.09	n.d.	n.d.
DL- <i>allo</i> -Isothreonine ^f (β)	0.87 ± 0.02	0.85 ± 0.08	0.084 ^d ± 0.004	0.16 ± 0.01	0.306 ± 0.008	0.68 ± 0.01	n.d.	n.d.
DL- β -Homoserine ^e (β)	0.51 ± 0.04	0.55 ± 0.04	0.098 ± 0.003	0.119 ± 0.009	0.40 ± 0.03	0.259 ± 0.006	n.d.	n.d.
D-3-A-2-HMPA ^g (β)	n.d.	0.26 ^d ± 0.02	n.d.	0.0102 ^d ± 0.002	n.d.	0.082 ± 0.003	n.d.	n.d.
L-4-A-2-HBA ^g (γ)	n.d.	0.8 ± 0.1	n.d.	0.38 ± 0.01	n.d.	0.37 ± 0.02	0.041 ± 0.003	0.040 ± 0.003
D-4-A-3-HBA (γ)	n.d.	0.34 ^d ± 0.03	n.d.	0.15 ^d ± 0.01	n.d.	0.090 ^d ± 0.003	0.017 ^d ± 0.001	n.d.
L-4-A-3-HBA (γ)	n.d.	0.20 ± 0.03	n.d.	0.12 ± 0.01	n.d.	0.073 ± 0.004	0.013 ± 0.002	n.d.
Total (nmol/g)	171 ± 1 ^g	144 ± 6 ^g	56 ± 3	148 ± 10	110 ± 10	168 ± 2	0.42 ± 0.01	10 ± 1
Sum of HW & HCl (nmol/g)	315 ± 6 ^g		200 ± 10		270 ± 10		10 ± 1	
HW / (HW + HCl)	54 %		27 %		39 %		4 %	

n.d. = value not determined due to trace amino acid abundances.

^a Sample extracts were analyzed by HFBA-isopropyl derivatization and GC-MS. The reported uncertainties (δx) are based on the standard deviation value (σ) of 2-3 separate measurements (n) with a standard error, $\delta x = \sigma_x \cdot (n)^{-1/2}$.

^b Minimum abundances are shown without an accompanying standard error because replicate measurements of this analyte were not made.

^c The enantiomers were not resolved by the chromatographic separation applied in this study.

^d The abundances presented here are approximate due to quantitative interferences posed by non-HAA, coeluting species in the meteorite sample.

^e The abundances were reported as the combined quantity estimates of both enantiomers because although the enantiomers were separated, the elution orders of the respective enantiomers were not determined due to a lack of enantiopure standard availability.

^f Precise abundance estimates are not provided due to the lack of enantiopure standards. Instead, upper limit abundances were estimated.

^g Total abundances were determined using individual HAA abundance estimates that were not accompanied by a standard error, which may cause the true uncertainties of the total abundance estimates to be larger than the total uncertainty estimates provided here.

Table 1-4. Summary of the combined abundances (nmol/g) of the three- to four-carbon hydroxy amino acids in the two extracts (HW + HCl extracts) of CM and CR carbonaceous chondrites measured by GC-MS^a.

	Y-791198 CM2 (CM2.4/ 1.6/1.5)	A-881458 CM2, very weakly heated	LEW 90500 CM2 (CM2.4/ 1.4/1.6)	LON 94101 CM2 (CM2.6/ 1.3/1.8)	ALH 83100 CM1/2 (CM2.1/ 1.2/1.1)	MIL 07525 CR2 (CR2.8)	LAP 02342 CR2 (CR2.8/ 2.7/2.5)	MET 00426 CR2 (CR2.8/ 2.6/2.6)	GRO 95577 CR1 (CR2.0/ 1.3/1.3)
Hydroxy amino acids (Amine position)	HW + HCl	HW + HCl	HW + HCl	HW + HCl	HW + HCl	HW + HCl	HW + HCl	HW + HCl	HW + HCl
D-Serine (α)	11 \pm 2 ^b	0.97 \pm 0.04	0.225 \pm 0.009	0.37 \pm 0.05	0.30 \pm 0.02	36 ^c	53 \pm 7	62 \pm 8	1.3 \pm 0.2
L-Serine (α)	28 \pm 4 ^b	3.8 \pm 0.3	0.94 \pm 0.07	2.8 \pm 0.5	6.1 \pm 0.2	39 ^c	54 \pm 7	69 \pm 10	6 \pm 1
DL-Isoserine ^e (β)	9.6 \pm 0.4	0.99 \pm 0.03	0.59 \pm 0.02	0.49 \pm 0.01	0.54 \pm 0.01	6.9 \pm 0.5	1.6 \pm 0.1	4.1 \pm 0.1	0.160 \pm 0.006
L- α -Methylserine (α)	20 \pm 1	1.50 \pm 0.07	0.882 \pm 0.009	0.47 \pm 0.03	0.160 \pm 0.004	95 \pm 4	33 \pm 3	53 \pm 1	0.067 \pm 0.004
D- α -Methylserine (α)	21 \pm 1	1.5 \pm 0.1	0.89 \pm 0.01	0.45 \pm 0.02	0.155 \pm 0.006	106 \pm 4	38 \pm 3	60 \pm 2	0.066 \pm 0.002
D-Threonine (α)	0.75 \pm 0.09	0.052 \pm 0.008	0.075 \pm 0.002	0.026 \pm 0.002	n.d.	4.2 ^e \pm 0.2	2.3 ^e \pm 0.2	2.1 ^e \pm 0.1	n.d.
L-Threonine (α)	1.8 \pm 0.2	0.97 \pm 0.04	0.183 \pm 0.004	0.54 \pm 0.05	2.01 \pm 0.06	4.5 \pm 0.2	2.6 ^e \pm 0.3	4.58 \pm 0.08	1.3 \pm 0.3
D- <i>allo</i> -Threonine (α)	0.36 ^e \pm 0.02	0.052 ^e \pm 0.005	0.071 ^e \pm 0.003	0.036 ^e \pm 0.002	0.068 ^e \pm 0.004	2.6 \pm 0.1	2.6 ^e \pm 0.8	1.9 ^e \pm 0.1	n.d.
L- <i>allo</i> -Threonine (α)	0.41 ^e \pm 0.04	0.053 ^e \pm 0.005	0.062 \pm 0.004	0.036 ^e \pm 0.002	0.068 \pm 0.004	3.2 ^e \pm 0.1	2.6 ^e \pm 0.8	2.12 ^e \pm 0.05	n.d.
D-Homoserine (α)	1.61 ^e \pm 0.08	0.41 \pm 0.02	0.163 ^e \pm 0.007	0.107 ^e \pm 0.009	0.058 \pm 0.001	2.8 ^e \pm 0.2	1.02 ^e \pm 0.04	2.48 ^e \pm 0.09	0.027 ^e \pm 0.002
L-Homoserine (α)	1.58 \pm 0.08	0.45 ^e \pm 0.01	0.163 ^e \pm 0.006	0.12 ^e \pm 0.01	0.134 \pm 0.002	2.6 ^e \pm 0.1	0.94 \pm 0.04	2.3 \pm 0.1	0.0518 ^e \pm 0.0008
DL- α -Methylisoserine ^e (β)	20.0 \pm 0.8	2.8 \pm 0.1	1.82 \pm 0.03	0.90 ^e \pm 0.03	0.105 \pm 0.008	4.7 ^e \pm 0.2	10 \pm 2	5.3 \pm 0.2	0.66 \pm 0.01
DL-Isothreonine ^f (β)	2.5 \pm 0.2	0.30 \pm 0.03	0.32 \pm 0.01	0.17 \pm 0.02	n.d.	3.7 \pm 0.3	0.81 \pm 0.06	3.1 \pm 0.1	n.d.
DL- <i>allo</i> -Isothreonine ^f (β)	1.61 \pm 0.05	0.184 \pm 0.009	0.170 \pm 0.006	0.127 \pm 0.007	0.019 \pm 0.002	1.72 \pm 0.09	0.24 ^e \pm 0.01	0.99 \pm 0.02	n.d.
DL- β -Homoserine ^e (β)	1.69 \pm 0.05	0.073 \pm 0.007	0.143 \pm 0.004	0.16 \pm 0.01	0.025 \pm 0.002	1.06 \pm 0.05	0.217 \pm 0.009	0.66 \pm 0.03	n.d.
D-3-A-2-HMPA ^g (β)	1.7 ^e \pm 0.2	0.24 ^e \pm 0.02	0.027 ^e \pm 0.002	0.034 ^e \pm 0.002	n.d.	0.26 ^e \pm 0.02	0.102 ^e \pm 0.002	0.082 \pm 0.003	n.d.
L-4-A-2-HBA ^g (γ)	2.30 ^e \pm 0.09	0.52 \pm 0.04	0.093 \pm 0.003	0.072 \pm 0.008	0.038 \pm 0.001	0.81 \pm 0.07	0.38 \pm 0.01	0.37 \pm 0.02	0.081 \pm 0.005
D-4-A-3-HBA (γ)	0.474 ^e \pm 0.005	0.13 ^e \pm 0.01	0.084 ^e \pm 0.001	0.062 ^e \pm 0.003	0.036 ^e \pm 0.002	0.34 ^e \pm 0.03	0.15 ^e \pm 0.01	0.090 ^e \pm 0.003	0.017 ^e \pm 0.001
L-4-A-3-HBA (γ)	0.37 \pm 0.01	0.10 \pm 0.01	0.044 \pm 0.002	0.031 \pm 0.002	0.0243 \pm 0.0008	0.20 \pm 0.03	0.12 \pm 0.01	0.073 \pm 0.004	0.013 \pm 0.002
Total of α -HAAs	85 \pm 5 ^h	9.9 \pm 0.3 ^h	3.65 \pm 0.08 ^h	4.9 \pm 0.5 ^h	9.0 \pm 0.2 ^h	296 \pm 6 ^h	190 \pm 10	260 \pm 10	9 \pm 1
Total of β -HAAs	37.1 \pm 0.9	4.6 \pm 0.1	3.07 \pm 0.04	1.89 \pm 0.04	0.69 \pm 0.02	18.4 \pm 0.6	13 \pm 2	14.2 \pm 0.3	0.82 \pm 0.01
Total of γ -HAAs	3.14 \pm 0.09	0.75 \pm 0.04	0.220 \pm 0.004	0.164 \pm 0.009	0.098 \pm 0.002	1.3 \pm 0.1	0.65 \pm 0.02	0.53 \pm 0.02	0.112 \pm 0.005
Sum of HW & HCl (nmol/g)	126 \pm 5 ^h	15.2 \pm 0.3 ^h	6.94 \pm 0.09 ^h	7.0 \pm 0.5 ^h	9.8 \pm 0.2 ^h	315 \pm 6 ^h	200 \pm 10	270 \pm 10	10 \pm 1

n.d. = value not determined due to trace amino acid abundances.

^a The combined abundances in the HW and HCl extracts were summed from Table 2 and 3, and the uncertainties ($\delta x_{\text{combined}}$) were propagated through the relevant equations with $\delta x_{\text{combined}} = (\delta x_{\text{HW}}^2 + \delta x_{\text{HCl}}^2)^{1/2}$.

^b Combined abundances were determined using individual HAA abundance estimates that were not accompanied by a standard error, which may cause the true uncertainties of the total abundance estimates to be larger than the total uncertainty estimates provided here.

^c Minimum abundances are shown without an accompanying standard error because replicate measurements of this analyte were not made.

^d The enantiomers were not resolved by the chromatographic separation applied in this study.

^e The abundances presented here are approximate due to quantitative interferences posed by non-HAA, coeluting species in the meteorite sample.

^f The abundances were reported as the combined quantity estimates of both enantiomers because although the enantiomers were separated, the elution orders of the respective enantiomers were not determined due to a lack of enantiopure standard availability.

^g Precise abundance estimates are not provided due to the lack of enantiopure standards. Instead, upper limit abundances were estimated.

^h Total abundances were determined using individual HAA abundance estimates that were not accompanied by a standard error, which may cause the true uncertainties of the total abundance estimates to be larger than the total uncertainty estimates provided here.

Table 1-5. Summary of D/L ratios and L-enantiomeric excesses (L_{ee}) measured for several α -hydroxy amino acids in the HW and HCl extracts of CM and CR chondrites^a.

	Y-791198		A-881458		LEW 90500		LON 94101		ALH 83100	
	(CM2.4/1.6/1.5)		(CM2, very weakly heated)		(CM2.4/1.4/1.6)		(CM2.6/1.3/1.8)		(CM2.1/1.2/1.1)	
	Hot water	HCl	Hot water	HCl	Hot water	HCl	Hot water	HCl	Hot water	HCl
	D/L ratio	D/L ratio	D/L ratio	D/L ratio	D/L ratio	D/L ratio	D/L ratio	D/L ratio	D/L ratio	D/L ratio
	(%Lee)	(%Lee)	(%Lee)	(%Lee)	(%Lee)	(%Lee)	(%Lee)	(%Lee)	(%Lee)	(%Lee)
Serine (α)	b	0.35 \pm 0.12 (47.9 \pm 10.0)	0.13 \pm 0.02 (76.8 \pm 1.7)	0.42 \pm 0.03 (40.8 \pm 2.1)	0.36 \pm 0.05 (47.0 \pm 4.2)	0.20 \pm 0.02 (66.9 \pm 2.0)	0.17 \pm 0.04 (70.3 \pm 4.1)	0.12 \pm 0.04 (78.4 \pm 4.0)	0.031 \pm 0.002 (93.9 \pm 0.3)	0.13 \pm 0.02 (76.6 \pm 1.9)
α -Methylserine (α)	1.06 \pm 0.15 (-2.7 \pm 7.2)	1.02 \pm 0.08 (-0.9 \pm 4.2)	1.03 \pm 0.11 (-1.5 \pm 5.3)	1.03 \pm 0.04 (-1.2 \pm 2.0)	1.02 \pm 0.02 (-1.0 \pm 0.9)	0.95 \pm 0.02 (2.4 \pm 0.8)	0.96 \pm 0.01 (1.9 \pm 0.6)	0.97 \pm 0.18 (1.4 \pm 9.1)	1.02 \pm 0.05 (-1.0 \pm 2.4)	0.95 \pm 0.05 (2.4 \pm 2.7)
Threonine (α)	0.65 \pm 0.16 (20.9 \pm 9.7)	0.30 \pm 0.06 (53.3 \pm 5.0)	0.15 \pm 0.02 (74.2 \pm 2.2)	0.02 \pm 0.01 (95.2 \pm 1.3)	0.57 \pm 0.02 (27.0 \pm 1.6)	0.18 \pm 0.01 (69.2 \pm 0.7)	0.11 \pm 0.01 (80.7 \pm 1.3)	0.032 \pm 0.005 (93.8 \pm 0.7)	c	c
<i>allo</i> -Threonine (α)	d	0.99 \pm 0.12 (0.3 \pm 6.2)	d	d	d	d	d	b	d	d
Homoserine (α)	d	d	0.96 \pm .06 (2.2 \pm 3.3)	d	d	1.00 \pm 0.07 (0.1 \pm 3.5)	d	0.86 \pm 0.17 (7.6 \pm 9.2)	0.32 \pm 0.01 (51.7 \pm 1.2)	0.85 \pm 0.03 (8.0 \pm 1.6)

	MIL 07525		LAP 02342		MET 00426		GRO 95577	
	(CR2.8)		(CR2.8/2.7/2.6)		(CR2.8/2.6/2.6)		(CR2.0/1.3/1.3)	
	Hot water	HCl	Hot water	HCl	Hot water	HCl	Hot water	HCl
	D/L ratio	D/L ratio	D/L ratio	D/L ratio	D/L ratio	D/L ratio	D/L ratio	D/L ratio
	(%Lee)	(%Lee)	(%Lee)	(%Lee)	(%Lee)	(%Lee)	(%Lee)	(%Lee)
Serine (α)	b	b	0.92 \pm 0.12 (4.2 \pm 6.2)	0.99 \pm 0.19 (0.5 \pm 9.5)	b	0.84 \pm 0.04 (8.6 \pm 1.9)	0.13 \pm 0.01 (76.6 \pm 1.4)	0.22 \pm 0.05 (64.2 \pm 5.3)
α -Methylserine (α)	1.11 \pm 0.02 (-5.4 \pm 0.8)	1.12 \pm 0.18 (-5.5 \pm 8.5)	1.18 \pm 0.16 (-8.1 \pm 7.3)	1.05 \pm 0.23 (-2.6 \pm 11.3)	1.10 \pm 0.09 (-4.9 \pm 4.3)	1.14 \pm 0.02 (-6.6 \pm 0.8)	0.94 \pm 0.09 (3.3 \pm 4.8)	1.00 \pm 0.08 (0.0 \pm 3.9)
Threonine (α)	d	d	d	d	d	d	c	c
<i>allo</i> -Threonine (α)	d	1.07 \pm 0.22 (-3.2 \pm 10.5)	d	d	d	d	n.d.	n.d.
Homoserine (α)	d	d	d	d	d	d	d	d

n.d. = not determined.

^a The standard errors (δx) for D/L ratios and the L-enantiomeric excesses (L_{ee}) are based on the values and errors from Table 2 and Table 3 propagated through the relevant equations with $L_{ee} = [(L-D)/(L+D)] \cdot 100$.

^b The L-enantiomeric excesses were not reported because replicate measurements of this analyte were not made.

^c The L-enantiomeric excesses could not be calculated because the concentration of the D-enantiomer was below the detection limit.

^d L-enantiomeric excesses were not reported due to coelution with other chromatographic peaks.

Chapter 2.

The Amino Acid Syntheses from Glycolaldehyde and Ammonia

2.1. Introduction

In Chapter 1, the HAA analyses revealed that the ammonia-involved formose-like reaction could proceed in the CM and CR chondrite parent bodies based on the ubiquitous detection of β - and γ -HAAs. Koga and Naraoka (2017) reported that various amino acids, including α -, β -, and γ -HAAs were synthesized from formaldehyde, acetaldehyde, glycolaldehyde, and ammonia in aqueous solution at 60 °C for 6 days. However, the detailed formation pathways of the amino acid synthesis remained unclear. Detection of the amino acids' precursor compound(s) should be essential to pursue the amino acid formation pathway. For instance, in the Strecker cyanohydrin reaction, α -aminonitriles correspond to a precursor compound to produce α -amino acids after hydrolysis. In this case, detection of α -aminonitriles with α -amino acids in the experimental product would be robust evidence that the resultant α -amino acids were produced via the precursor α -aminonitriles by the Strecker cyanohydrin reaction. Hence, in this study, an amino acid synthesis experiment using glycolaldehyde and ammonia (more straightforward starting materials than those of Koga and Naraoka (2017)) was performed to detect amino acids and search the corresponding precursor compound(s) to determine how the ammonia-involved formose-like reaction can produce amino acids.

2.2. Materials and Methods

2.2.1. Chemicals and Reagents

Commercial standards of amino acids were purchased from various manufacturers as follows: Sigma: glycine (>99 % purity), Aldrich: D,L-alanine (>99 % purity), β -Alanine (>99 % purity), Wako: D,L-serine (>98 % purity), and TCI: D,L-isoserine (>98 % purity), D,L-homoserine (>98 % purity). A stock mixed amino acid solution was prepared by combining individual amino acid standards described above in Milli-Q water. Commercial standards of other organic compounds were obtained from several manufacturers as follows: TCI: D,L-glyceric acid (~20 % in water), Combi-Blocks: L-threonic acid calcium salt (>95 % purity), and Sigma-Aldrich: N-oxalylglycine (>98 % purity). A stock solution of 3-fluoro-L-tyrosine (TCI, >98 % purity) was prepared as an internal standard.

The amino acid synthesis experiment was performed using ammonia solution (Wako, 29.5 %) and [1,2- ^{13}C]glycolaldehyde (Omicron Biochemicals, Inc., 99 atom-% ^{13}C). The ^{13}C -labeled glycolaldehyde enabled us to obtain ^{13}C -labeled organic compounds that could be confirmed as the reaction products but not procedural contamination. Acid-hydrolysis was performed using HCl (Wako, for Amino Automated Analysis, 35.0~37.0 %). Pre-column derivatization of samples before GC-MS analyses involved the use of acetyl chloride (TCI, >98 % purity), isopropanol (Wako, Super Dehydrated, >99.7 % purity), HFBA (TCI, >95 % purity), chloroform (TCI, for HPLC, >99.5 %), and anhydrous sodium sulfate (Wako, heated at 500 °C before the use). All glassware and sample handling tools were rinsed with Milli-Q ultrapure water, wrapped in aluminum foil, and then heated at 500 °C, in air, overnight.

2.2.2. Experimental Amino Acid Synthesis and Sample Preparation

Fig. 2-1 shows a schematic diagram of the amino acid synthesis experiment conducted in this study. The plausibility of experimental conditions employed here will be discussed in the following chapter (Chapter 3). Aqueous solutions were prepared by mixing ammonia solution and ^{13}C -labeled glycolaldehyde in Milli-Q water with the molar ratio of 1000/10/1 for H_2O /ammonia/glycolaldehyde, respectively. The aqueous solution (~3 mL, pH 11.6) was heated at 60 °C for 6 days in the air or nitrogen-purged glass ampoules to evaluate the effect of free oxygen for the amino acid synthesis in the reaction. After heating, the sealed ampoules were cooled to room temperature and opened. Hereafter, the experimental products synthesized under air or nitrogen atmosphere will be referred to as the air-product or N_2 -product, respectively. A 100 μL of each product was separately transferred to another glass ampoule, dried under vacuum, and were subjected to a 6 M HCl hydrolysis procedure at 105 °C for 24 h to determine total acid-hydrolyzable amino acid abundances that include both free amino acids and bound-form amino acids synthesized by the acid-hydrolysis from the precursor compounds. Another 100 μL of each air- and N_2 product was not subjected to the acid-hydrolysis to determine non-hydrolyzed free amino acids' abundances.

For GC-MS analysis of the amino acids, both the non-hydrolyzed and acid-hydrolyzed fractions were subjected to HFBA-isopropyl derivatization using the following protocol: 1) esterification with 160 μL of isopropanol and 40 μL of acetyl chloride at 80 °C for 3 h, 2) acylation with 50 μL of HFBA at 80 °C for 100 min, 3) removal of excess acids by mixing with Milli-Q water and chloroform, and 4) removal of water from chloroform using anhydrous sodium sulfate before injection into the GC-MS system. Procedural blanks composed of Milli-Q water were prepared using the identical

extraction and processing protocols as the experimental product and analyzed to provide background-corrected abundance estimates of target analytes. An internal standard of 3-fluoro-L-tyrosine was added to the experimental product and procedural blanks before the HFBA-isopropyl derivatization.

For the amino acid precursor analysis, the non-hydrolyzed fraction of the air-products was subjected only to isopropyl-ester derivatization (without HFBA-derivatization) as the similar procedure described above. The commercial standard of N-oxalylglycine was derivatized and analyzed in the same manner as the experimental product.

2.2.3. GC-MS Analysis

The HFBA-isopropyl or isopropyl derivatives of targeted analytes were analyzed using a Thermo Trace GC and Thermo Finnigan Polaris-Q mass spectrometer. Chromatographic separation was achieved using a 5 m base-deactivated fused silica guard column (Restek) in series with two 25 m CP-Chirasil-Dex CB columns (Agilent). A helium flow rate of 2.0 mL/min, and the following temperature program was employed during chromatographic separation: initial oven temperature was 50 °C and was held for 2 min, followed by ramping at 20 °C/min to 110 °C and held for 20 min, followed by ramping at 20 °C/min to 130 °C, and finally ramping at 5 °C/min to 200 °C and held for 1 min. The mass spectrometer was performed in full scan mode from m/z 50–510. Amino acids were quantified by comparing the procedural blank-subtracted mass chromatographic peak areas in the experimental product to those in the analytical standard. The amino acids' peak areas were corrected based on the peak area of the 3-fluoro-L-tyrosine internal standard to minimize analytical errors between each GC-MS analysis (typical injection volume was 1 μ L). The amino acid concentration was calculated relative

to the starting glycolaldehyde's molar ratio (ppm, 10^{-6}).

2.3. Results and Discussion

2.3.1. A Comparison of Molecular Distributions between the Air- and N₂-Products.

Fig. 2-2 shows the total ion chromatograms (m/z 50–510) obtained from the non-hydrolyzed air- and N₂-products. A comparison of the two chromatograms exhibits that the peak intensities of glyceric acid (peak #1), threonic acid (peak #2), and glycine (peak #3) significantly increased in the air-product than those of the N₂-product, indicating that oxygen in air atmosphere involved reactions to produce these organic compounds. In particular, sugar acids such as glyceric acid (C₃H₆O₄) and threonic acid (C₄H₈O₅) can be produced by the oxidation of glyceraldehyde (C₃H₆O₃) and threose (C₄H₈O₄), respectively, which are synthesized by polymerization of the starting material, glycolaldehyde (C₂H₄O₂). Thus, the presence of sugar acids indicates that oxygen in air atmosphere involved oxidation during the synthesis of product compounds, which significantly increased under air atmosphere, including the amino acid glycine (see the peak #3 in **Fig. 2-2**).

Table 2-1 shows the average molar ratio of synthesized amino acids relative to starting glycolaldehyde in the air- and N₂-products. This study investigated the abundance of glycine, alanine, β-alanine, serine, isoserine, and homoserine in their non-hydrolyzed (free) and acid-hydrolyzed (free + bound) fractions. **Fig. 2-3** illustrated the amino acids' abundances in the air- and N₂-products from **Table 2-1**. The figure demonstrated that more abundant amino acids were detected in the air-product than the N₂-product, indicating that oxygen in air atmosphere also proceeded with the amino acids' syntheses, similar to sugar acids described above (**Fig. 2-2**). The most abundant amino acid was glycine, and the concentration was the largest in the acid-hydrolyzed fraction of the air-product, 4150 ± 70 parts per million (ppm) by mol relative to the starting glycolaldehyde

(**Table 2-1**). The abundance of glycine in the non-hydrolyzed air-product (2560 ± 20 ppm) was approximately 10.5 times larger than that in the non-hydrolyzed N₂-product (244 ± 1 ppm). The abundance ratios of amino acids in the air-product relative to the N₂-product ranged from 1.14 for homoserine to 13.5 for serine, both in the non-hydrolyzed fraction.

2.3.2. A Detection of ¹³C-Labeled N-Oxalylglycine in the Air-Product.

As a candidate for the precursor compound of glycine, which was the most abundant amino acid in the experimental products, the presence of N-oxalylglycine was investigated in the non-hydrolyzed air-product. **Fig. 2-4** demonstrates that ¹³C-labeled N-oxalylglycine was detected in the air-product based on the comparisons of the retention time (38.9 min) and the mass spectra with the ¹²C-commercial standard N-oxalylglycine. The isopropyl-ester derivatized ¹²C-N-oxalylglycine shows a fragment ion pattern consisting of *m/z* 102 (the base peak), 74, 172, and 144 (in the order of the relative intensity). These ions contain a different number of carbon atoms derived from the parent N-oxalylglycine. For instance, the fragmental ion of *m/z* 102 possesses 3 carbon atoms from the parent, as shown in the extracted ion chromatogram of (B) in **Fig. 2-4**. Thus, when the carbon atoms are substituted by ¹³C, the ion mass will increase to *m/z* 105 along with the number of carbon atoms derived from N-oxalylglycine. Thus, the isopropyl-ester derivative of ¹³C-N-oxalylglycine possesses fragmental ions of *m/z* 105, 76, 176, and 147 (see the structures of fragment ions shown in the mass spectra of (A) and (B) in **Fig. 2-4**). These ions were detected in the non-hydrolyzed air-product at the same retention time (38.9 min) as that of the commercial standard N-oxalylglycine, indicating that N-oxalylglycine was produced during glycine synthesis in this experiment. The concentration of ¹³C-N-oxalylglycine was 910 ± 70 ppm by mol relative to the starting glycolaldehyde. During the HFBA-isopropyl derivatization, N-oxalylglycine can be

transformed into the HFBA-isopropyl glycine derivative in the same manner as free glycine in the reaction product. Hence, the abundance of ^{13}C -N-oxalylglycine (910 ± 70 ppm) corresponded to 36% of the free glycine found in the non-hydrolyzed air-product (2560 ± 20 ppm, **Table 2-1**), indicating that N-oxalylglycine was the primary precursor compound of glycine in this reaction product. This observation provides robust evidence to reveal how amino acids are synthesized from glycolaldehyde and ammonia via the ammonia-involved formose-like reaction, as discussed in the following section.

2.3.3. The Formation Pathway of Glycine via N-Oxalylglycine: Implications for Amino Acid Syntheses by the Ammonia-Involved Formose-like Reaction.

The plausible formation pathway of glycine from glycolaldehyde and ammonia in this experiment is described in **Fig. 2-5**. The presence of N-oxalylglycine in the air-product (**Fig. 2-4**) supports that this formation pathway proceeded in this experiment. Yanagawa et al. (1982, 1984) reported that the N-oxalylglycine could be produced from glyoxylic acid and ammonia under acidic or neutral conditions. As this experiment was conducted under alkaline conditions (pH 11.6), the formation of N-oxalylglycine from glyoxylic acid and ammonia could proceed as described in **Fig. 2-5** (2), based on the formation pathway proposed by Yanagawa et al. (1982, 1984). The synthesis of N-oxalylglycine is followed by hydrolysis, yielding the resultant amino acid glycine and the byproduct of oxalic acid in **Fig. 2-5** (3). It is worth noting that glyoxylic acid can be produced from the oxidation of glycolaldehyde, which is the starting organic compound in this experiment (**Fig. 2-5** (1)). Glycolaldehyde can be oxidized by oxygen in air atmosphere to produce glyoxylic acid. Thus, the increase of glycine's abundance in the air-product compared to the N_2 -product (**Table 2-1** and **Fig. 2-3**) may indicate an increase of glyoxylic acid content by the effect of oxygen. Therefore, the synthesis of glycine by

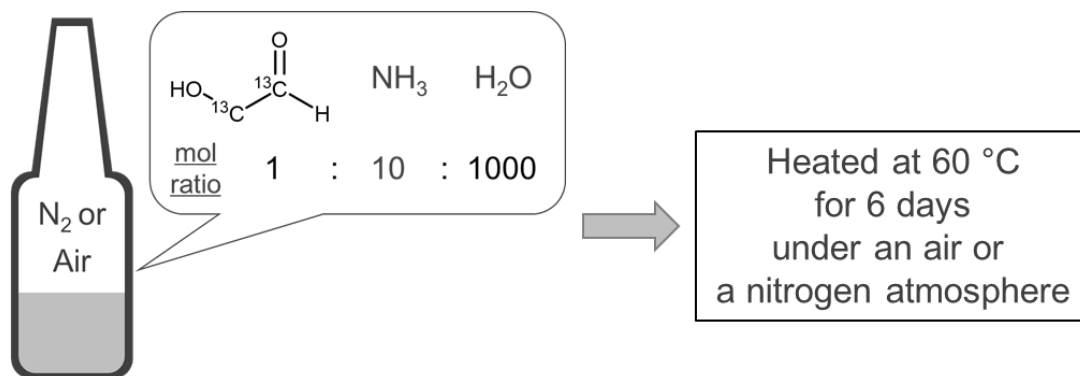
the ammonia-involved formose-like reaction can be described as followed: (1) glycolaldehyde is oxidized to be glyoxylic acid, (2) reacting with ammonia to produce N-oxalylglycine, (3) followed by hydrolysis for yielding resultant glycine (**Fig. 2-5**).

The formation mechanism of glycine in this experiment can be generalized as the reaction between oxoacid (*e.g.*, glyoxylic acid) and ammonia, which might be applied to the formation mechanisms of other amino acids synthesized in the experimental products. For instance, the reaction between hydroxypyruvic acid (α -oxo acid) and ammonia could produce serine (α -HAA) as the same formation mechanism for glycine (**Fig. 2-6**). Besides, isoserine (β -HAA) and 4-A-2-HBA (γ -HAA) could also be formed from the reactions of ammonia and β -oxoacid (2-Hydroxy-3-oxopropanoic acid) and γ -oxoacid (2-Hydroxy-4-oxobutanoic acid), respectively. Therefore, it can be hypothesized that the reaction between oxoacids and ammonia could produce various amino acids, including α -, β -, and γ -HAAs found in carbonaceous chondrites (Chapter 1); thus, the ammonia-involved formose-like reaction could be considered a formation mechanism that can comprehensively explain the distribution of meteoritic amino acids. Further investigations are needed to demonstrate these formation pathways for α -, β -, and γ -HAAs by detecting the intermediate compounds of α -, β -, and γ -oxoacids and the corresponding precursor compounds similar to N-oxalylglycine in the experimental products (**Fig. 2-6**). A comparison of molecular distributions of oxoacids and dicarboxylic acids (*e.g.*, oxalic acid is the byproduct of glycine production in **Fig. 2-5**) with those of amino acids will be necessary to evaluate how much the proposed formation pathways proceeded in the conditions of meteorite parent bodies during aqueous alteration.

2.4. Conclusion

This study conducted the amino acid synthesis experiment using ^{13}C -labeled glycolaldehyde and ammonia to reveal the detailed formation pathways of amino acids by the ammonia-involved formose-like reaction that could occur and produce HAAs found in carbonaceous chondrites. This experiment showed that the abundance of amino and sugar acids increased under air atmosphere than nitrogen atmosphere, indicating the effects of oxygen on their production. This observation implies that oxidation is an important step for proceeding with the ammonia-involved formose-like reaction. This study also revealed that the air-product contained ^{13}C -labeled N-oxalylglycine as a precursor compound of glycine in this experiment. The N-oxalylglycine is considered to be produced from glyoxylic acid and ammonia under alkaline condition, as similarly suggested by Yanagawa et al. (1982, 1984). The proposed formation pathway is consistent with the observation that the abundance of glycine increased significantly because of the effects of oxygen (~10.5 times at maximum) because glyoxylic acid, which is needed to synthesize N-oxalylglycine, can be produced by glycolaldehyde oxidation. Finally, N-oxalylglycine's formation pathway gives us a hypothesis that amino acids synthesized in this experiment could be produced from the reactions between corresponding isomers of oxoacids and ammonia. If this hypothesis is true, it is possible to describe the formation pathways of α -, β -, and γ -amino acids from corresponding α -, β -, and γ -oxoacids and ammonia, and the ammonia-involved formose-like reaction could be considered as a formation mechanism that can comprehensively explain the distribution of meteoritic amino acids, including HAAs found in CM and CR chondrites.

2.5. Figures



Glass Ampoule

Fig. 2-1. A schematic diagram of the amino acid synthesis experiment conducted in this study.

A glass ampoule was sealed under air or nitrogen atmosphere to evaluate the effect of oxygen for the syntheses of organic compounds, including amino acids.

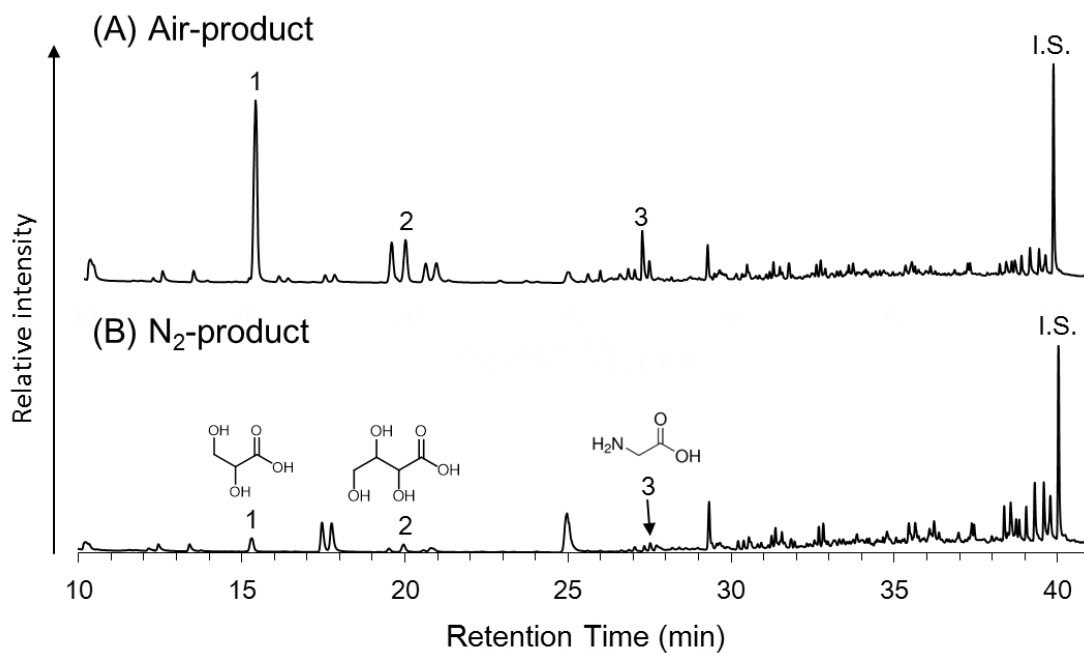


Fig. 2-2. A comparison of the 10–40 min regions of the GC-MS total ion chromatograms (m/z 50–510) obtained from the non-hydrolyzed (A) air- and (B) N_2 -products.

Peak identifications are as follows: (1) DL-glyceric acid (the enantiomer was not dissolved by the applied method); (2) L-threonic acid; (3) glycine; and (I.S.) internal 3-fluoro-L-tyrosine standard. The corresponding chemical structures for (1)–(3) are shown on each number in the chromatogram of (B). The intensities of peak (1)–(3) can be compared between (A) and (B) because a similar intensity of I.S. was obtained in both samples.

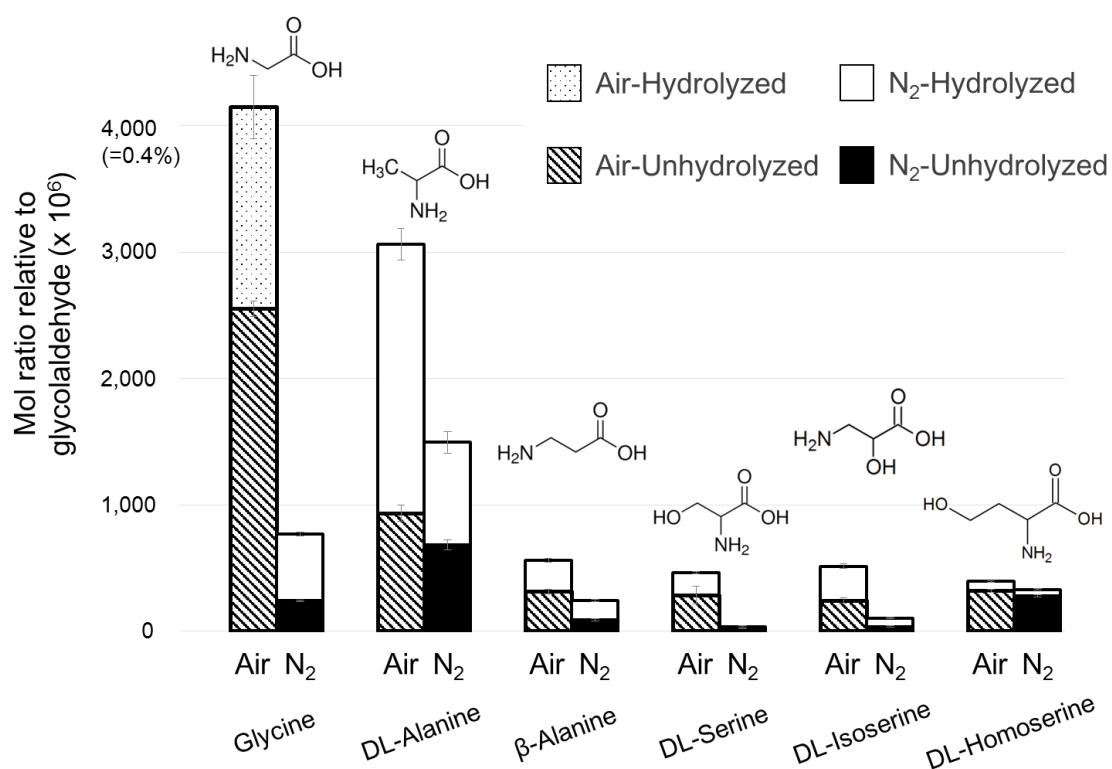


Fig. 2-3. A comparison of the molar ratios of amino acids in the air- and N₂-products relative to starting glycolaldehyde.

This figure is made from the data in **Table 2-1**. The corresponding chemical structures for amino acids are shown on each group of two bars obtained from the air- and N₂ products.

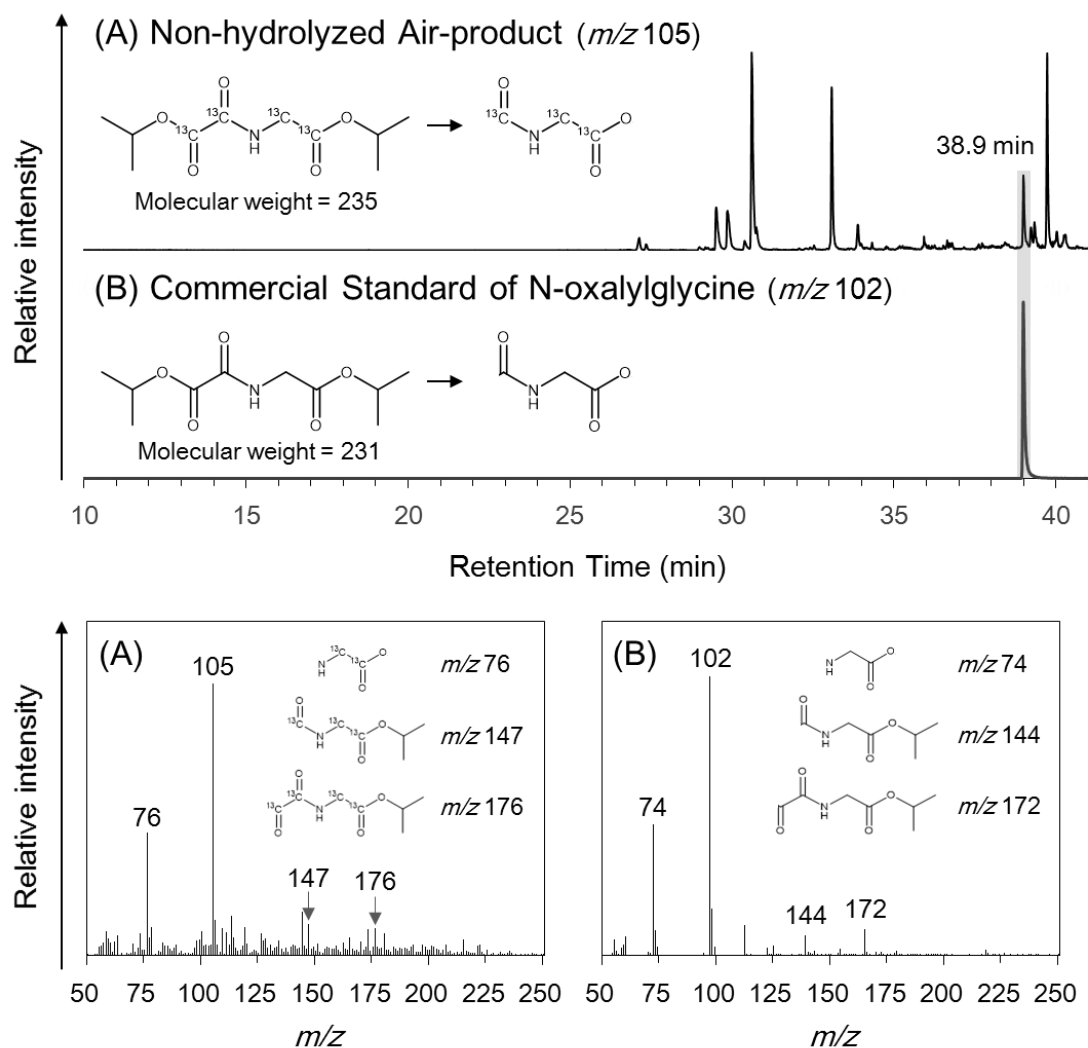
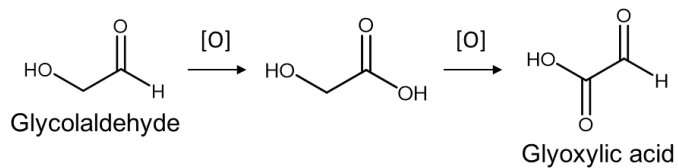


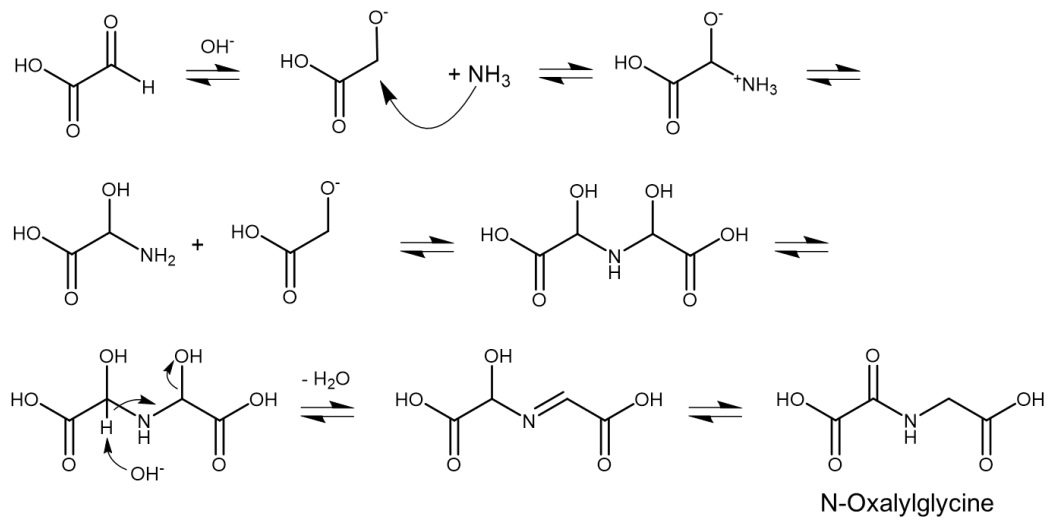
Fig. 2-4. Comparisons of the 10–41 min regions of the GC-MS extracted ion chromatograms of the base peaks of the isopropyl-ester derivatized (A) ^{13}C -labeled air-product (m/z 105) and (B) commercial standard ^{12}C -N-oxalylglycine (m/z 102) and their mass spectrums (m/z 50–250).

The mass spectra of the peak eluting at 38.9 min in the air-product corresponded to the ^{13}C -labeled N-oxalylglycine isopropyl-ester derivative, which was determined based on the fragmental ion pattern compared to that of the commercial standard (see the text for the detailed explanation).

(1) Oxidation of glycolaldehyde



(2) Formation of N-oxalylglycine from glyoxylic acid and ammonia



(3) Hydrolysis of N-oxalylglycine for producing glycine

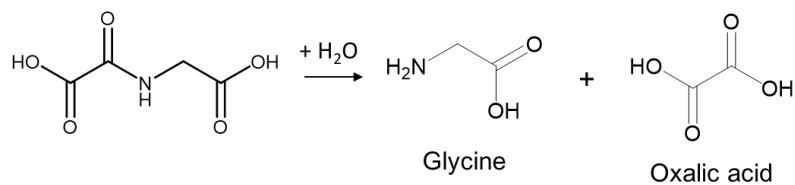


Fig. 2-5. The plausible formation pathway of glycine from glycolaldehyde and ammonia via the synthesis of N-oxalylglycine under alkaline condition.

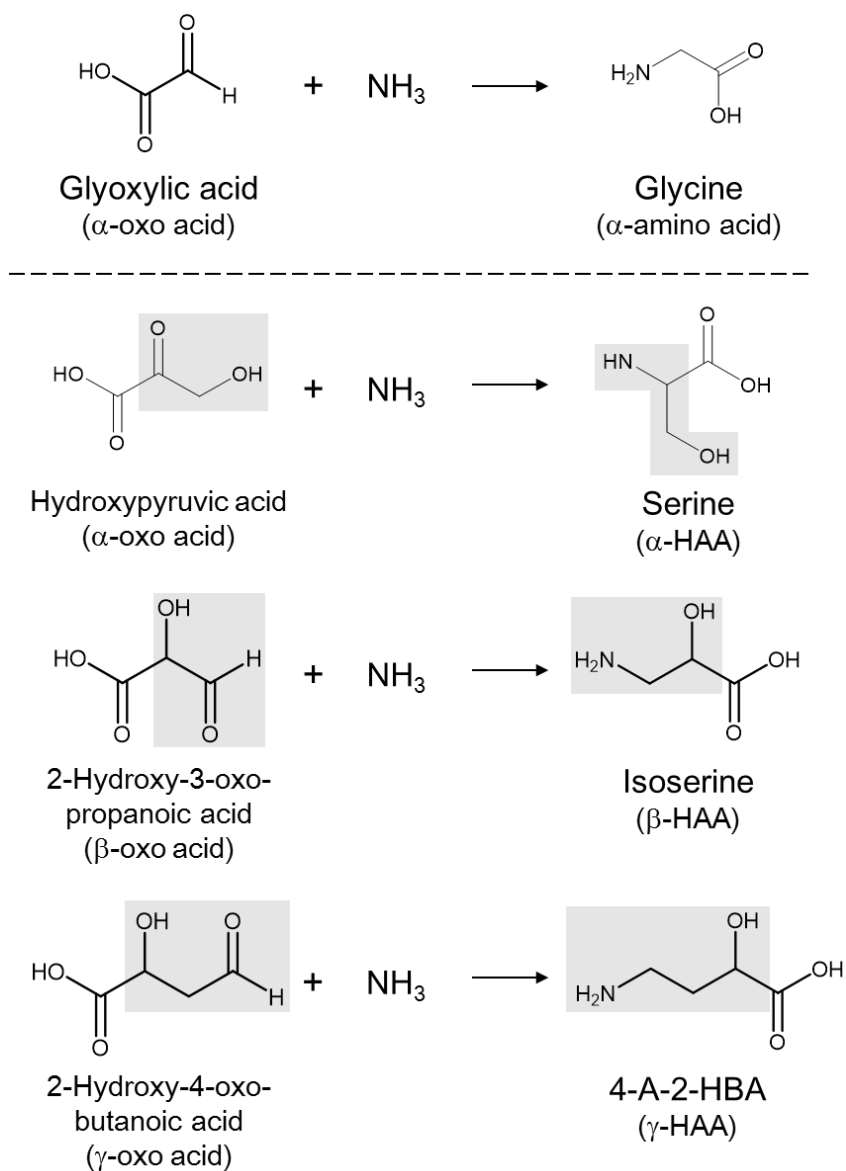


Fig. 2-6. The possible formation pathways of α -, β -, and γ -amino acids from the corresponding oxoacids and ammonia based on the formation of glycine from glyoxylic acid and ammonia.

2.6. Tables

Table 2-1. The concentrations of amino acids relative to starting glycolaldehyde (ppm by mol) in the non-hydrolyzed (free) and 6 M HCl hydrolyzed (total) air- and N₂ products^a.

C#	Amine position	Amino acids	Air-product			N ₂ -product			Air- / N ₂ -product	
			Free	Total	Increase by Hydrolysis	Free	Total	Increase by Hydrolysis	Free	Total
C ₂	α	Glycine	2560 ± 20	4150 ± 70	38%	244 ± 1	773 ± 5	69%	10.5	5.37
C ₃	α	DL-Alanine	1322 ± 9	3070 ± 40	57%	970 ± 10	1500 ± 30	35%	1.36	2.05
	β	β-Alanine	315 ± 1	564 ± 4	44%	89 ± 3	244 ± 3	63%	3.5	2.31
	α	DL-Serine	403 ± 4	465 ± 3	13%	30.0 ± 0.3	40 ± 2	25%	13.5	12
C ₄	β	DL-Isoserine	178 ± 3	256 ± 5	30%	28.8 ± 0.4	55 ± 1	47%	6.18	4.7
	α	DL-Homoserine	321 ± 3	395 ± 1	19%	283 ± 3	334 ± 2	15%	1.14	1.18
Total			5100 ± 20	8890 ± 80	43%	1640 ± 10	2941 ± 25	44%		

^a Sample extracts were analyzed by HFBA-isopropyl derivatization and GC-MS. The reported uncertainties (dx) are based on the standard deviation value (σ_x) of 3 separate measurements (n) with a standard error, $dx = \sigma_x \cdot (n)^{-1/2}$.

Chapter 3.

Amino Acid Syntheses from Glycolaldehyde and Ammonia in the Meteorite Parent Bodies

In this chapter, the distributions of HAAs in the CM and CR chondrites (Chapter 1) are compared with those of the experimental products of the amino acid syntheses from glycolaldehyde and ammonia (Chapter 2). **Table 3-1** summarized the abundance ratios of serine (Ser, C₃- α -HAA) to isoserine (IsoSer, C₃- β -HAA) calculated from **Table 1-2** and **Table 1-3** for the CM and CR chondrites, respectively, and **Table 2-1** for the experimental products. The Ser/IsoSer ratios for the meteorites were calculated as (D-serine x 2) / DL-isoserine to remove the effects of terrestrial contamination for L-serine. As a result, the Ser/IsoSer ratios obtained from the HW and HCl extracts of the CM chondrites ranged from 0.76 ± 0.04 of LEW 90500 to 2.2 ± 0.3 of Y-791198, which fell within the range of those of the experimental products, ranging from 0.73 ± 0.03 (acid-hydrolyzed N₂-product) to 2.27 ± 0.04 (non-hydrolyzed air-product). In contrast, the Ser/IsoSer ratios obtained from the CR chondrites showed significantly larger than the range (the maximum values were 66 ± 8 of the HW and HCl extracts of LAP 02342), except for the HW extract of GRO 95577 (0.39 ± 0.02). These results might imply that a similar synthetic process with the ammonia-involved formose-like reaction could have been more prevalent in the CM chondrites' parent bodies than the CR chondrites.

The amino acid synthesis experiment of this study was conducted using a molecular composition as starting materials, which was observed and estimated data of previous studies. The ratio of H₂O/ammonia/glycolaldehyde (1000/10/1 by mol) was referred from the observed cometary ice compositions; the ratio of H₂O/ammonia in

comet Halley was 100/0.1–2.0 (by %) (Ehrenfreund and Charnley 2000), and the ratio of H₂O/glycolaldehyde in the comet Lovejoy was 100/0.016 (by %) (Biver et al. 2015). The starting solution exhibited a pH value of 11.6, a similar pH value estimated for aqueous fluids in asteroids, ranging from 11.7 to 12.7 depending on different parameters (*e.g.*, temperature, water/rock ratio, initial CO₂ concentration) using thermodynamic calculations based on the oxygen isotopic compositions of calcite (Guo and Eiler 2007). The heating temperature of 60 °C was adapted from the estimated aqueous alteration temperature of ~80 °C (Baker et al. 2002) and 20–33 °C (Guo and Eiler 2007) for the CM2 Murchison meteorite. Therefore, the results of this study might support that the ammonia-involved formose-like reaction occurred in the conditions of CM chondrite parent bodies.

A significant implication obtained from the amino acid synthesis of this experiment is that the ammonia-involved formose-like reaction requires oxidation of starting aldehydes (*i.e.*, glycolaldehyde) for the amino acid syntheses, and free oxygen in air could promote the reactions (see **Fig. 2-5**). Although abundant molecular oxygen was found in the coma of comet 67P/Churyumov–Gerasimenko (Bieler et al. 2015), it remains unknown how much molecular oxygen was available in the environments of carbonaceous chondrite parent bodies. Alternatively, it might be possible that other oxidizing reagents drove the oxidation of aldehydes in the meteorite parent body. The hydroxy radicals produced by photolysis and radiolysis of H₂O is a candidate for oxidizing reagents (Gligorovski et al. 2015). The more oxidizing conditions of CM chondrite parent bodies than CR chondrites supported by the elemental distributions (Le Guillou et al. 2014; Orthous-Daunay et al. 2010), mineralogies (Howard et al. 2015; Naraoka and Hashiguchi 2019), and N-heterocyclic compounds' distribution (Naraoka

and Hashiguchi 2019) might imply the existence of molecular oxygen and/or other oxidizing reagents. Further investigations are needed to reveal the relationship between the predominance of the ammonia-involved formose-like reaction and the oxidizing conditions promoted by molecular oxygen and/or other oxidizing reagents in the meteorite parent body.

The experiments of amino acid synthesis from glycolaldehyde and ammonia revealed that the ammonia-involved formose-like reaction could produce sugar acids as the byproducts of the amino acid syntheses. The abundances of sugar acids and sugar in the CM2 Murchison meteorite were reported by Cooper and Rios (2016) and Furukawa et al. (2019), respectively. The total abundance of C₅-sugar acids was 1.3 x 10⁶ times larger than that of C₅-sugars (2943 pmol/g vs. 2.2 nmol/g, respectively). The larger abundances of sugar acids relative to sugar indicate that sugars could be transformed into sugar acids under oxidizing conditions of the CM2 Murchison meteorite parent body, which might be favorable for promoting the ammonia-involved formose-like reaction. Besides, the amino acid synthesis experiment suggested that oxoacids (*e.g.*, glyoxylic acid) were critical intermediates for the amino acid synthesis (**Fig. 2-5**). Although several keto acids were detected in the CM2 Murchison and ALH 83102 meteorite (Cooper et al. 2011), the distributions of oxoacids have not been well understood. Therefore, future investigations of sugar, sugar acids, and oxoacids in the CM and CR chondrites will give us clues about how much the ammonia-involved formose-like reaction could proceed in the conditions of meteorite parent bodies.

In conclusion, this paragraph summarizes the results and discussion in Chapters 1 and 2 according to the timeline of the syntheses of meteoritic HAAs from interstellar environments to carbonaceous chondrite parent bodies. First, the radical chemistry of

more abundant methanol than ethanol in the interstellar ices (Bisschop et al. 2008; Zhou et al. 2020) could be one potential explanation for more abundant α -methylserine and serine than other α -HAAs detected in the CM and CR chondrites studied here. Second, in the early stage of the aqueous alteration process in the meteorite parent body, the Strecker cyanohydrin reaction could proceed to produce α -amino acids. The detection of significantly abundant α -HAAs in the CR2 chondrites studied here can be explained by the dependency on ammonia concentrations of the Strecker cyanohydrin reaction (Peltzer et al. 1984) and the presence of more abundant ammonia in CR2 chondrites than the CM2 Murchison meteorite (Pizzarello et al. 2011). Thirdly, as the consumption of HCN in the meteorite parent body, meteoritic amino acid syntheses could transit from the Strecker cyanohydrin reaction to the ammonia-involved formose-like reaction (Koga and Naraoka 2017). This formation mechanism could occur to a similar degree in the CM and CR chondrites because these carbonaceous chondrites contained a similar range of β - and γ -HAAs. It can be hypothesized that α -, β -, and γ -HAAs could be produced from ammonia and corresponding α -, β -, and γ -oxo acids formed by the oxidation of aldehydes, which is similar to the formation pathway of glycine via N-oxalylglycine (Yanagawa et al. 1982, 1984). Thus, the ammonia-involved formose-like reaction could comprehensively explain the formation of various amino acid isomers in carbonaceous chondrites. Therefore, this study suggests that the ammonia-involved formose-like reaction could be a complementary formation mechanism of meteoritic amino acids with previously proposed mechanisms such as the Strecker cyanohydrin reaction.

3.1. Tables

Table 3-1. The abundance ratios of serine to isoserine in the CM and CR chondrites and the experimental products from glycolaldehyde and ammonia^a.

	(D-Serine x 2) / DL-Isoserine		
	HW	HCl	HW + HCl
<i>CM chondrites</i>			
Yamato 791198 CM2 (CM1.6/1.5)	6.0 ± 0.1	1.6 ± 0.3	2.2 ± 0.3
Asuka 881458 CM2, very weakly heated	1.1 ± 0.1	2.9 ± 0.3	2.0 ± 0.1
LEW 90500 CM2 (CM1.4/1.6)	0.40 ± 0.03	1.8 ± 0.1	0.76 ± 0.04
LON 94101 CM2 (CM1.3/1.8)	0.60 ± 0.07	4.1 ± 0.6	1.5 ± 0.2
ALH 83100 CM1/2 (CM1.2/1.1)	2.4 ± 0.1	0.7 ± 0.1	1.1 ± 0.1
<i>CR chondrites</i>			
MIL 07525 CR2 (CR2.8)	14.8 ± 0.9	9.1 ± 0.8	10.3 ± 0.7
LAP 02342 CR2 (CR2.8/2.7/2.5)	9.0 ± 0.8	90 ± 10	66 ± 8
MET 00426 CR2 (CR2.8/2.6/2.6)	50 ± 10	25 ± 1	30 ± 3
GRO 95577 CR1 (CR2.0/1.3/1.3)	0.39 ± 0.02	35 ± 4	17 ± 2
	DL-Serine / DL-Isoserine		
<i>Experimental products</i>	Free	Total	
Air-product	2.27 ± 0.04	1.82 ± 0.03	
N ₂ -product	1.04 ± 0.02	0.73 ± 0.03	

^a The ratios of serine to isoserine and standard errors (δx) are calculated based on the values and errors from **Table 1-2** and **Table 1-3** for the CM and CR chondrites, respectively, and **Table 2-1** for the experimental products. The ratios for meteorites were calculated as (D-serine x 2) / DL-isoserine to remove the effects of terrestrial contamination for L-serine.

References

- Alexander C. M. O. D., Howard K. T., Bowden R., and Fogel M. L. 2013. The classification of CM and CR chondrites using bulk H, C and N abundances and isotopic compositions. *Geochimica et Cosmochimica Acta* 123:244–260.
- Aponte J. C., Elsila J. E., Glavin D. P., Milam S. N., Charnley S. B., and Dworkin J. P. 2017. Pathways to Meteoritic Glycine and Methylamine. *ACS Earth and Space Chemistry* 1:3–13.
- Bada J. L., Glavin D. P., McDonald G. D., and Becker L. 1998. A Search for Endogenous Amino Acids in Martian Meteorite ALH84001. *Science* 279:362–365.
- Baker L., Franchi I. A., Wright I. P., and Pillinger C. T. 2002. The oxygen isotopic composition of water from Tagish Lake: Its relationship to low-temperature phases and to other carbonaceous chondrites. *Meteoritics & Planetary Science* 37:977–985.
- Bieler A. et al. 2015. Abundant molecular oxygen in the coma of comet 67P/Churyumov–Gerasimenko. *Nature* 526:678–681.
- Bisschop S. E., Jørgensen J. K., Bourke T. L., Bottinelli S., and van Dishoeck E. F. 2008. An interferometric study of the low-mass protostar IRAS 16293-2422: small scale organic chemistry. *Astronomy & Astrophysics* 488:959–968.
- Biver N. et al. 2015. Ethyl alcohol and sugar in comet C/2014 Q2 (Lovejoy). *Science Advances* 1:e1500863.
- Botta O., and Bada J. L. 2002. Extraterrestrial organic compounds in meteorites. *Surveys in Geophysics* 23:411–467.
- Breslow R. 1959. On the mechanism of the formose reaction. *Tetrahedron Letters* 1:22–26.
- Chimiak L., Elsila J. E., Dallas B., Dworkin J. P., Aponte J. C., Sessions A. L., and Eiler J. M. 2021. Carbon isotope evidence for the substrates and mechanisms of prebiotic synthesis in the early solar system. *Geochimica et Cosmochimica Acta* 292:188–202.
- Chyba C., and Sagan C. 1992. Endogenous production, exogenous delivery and impact-shock synthesis of organic molecules: an inventory for the origins of life. *Nature* 355:125–132.
- Cooper G. W., and Cronin J. R. 1995. Linear and cyclic aliphatic carboxamides of the Murchison meteorite: Hydrolyzable derivatives of amino acids and other carboxylic acids. *Geochimica et Cosmochimica Acta* 59:1003–1015.
- Cooper G., Reed C., Nguyen D., Carter M., and Wang Y. 2011. Detection and

- formation scenario of citric acid, pyruvic acid, and other possible metabolism precursors in carbonaceous meteorites. *Proceedings of the National Academy of Sciences* 108:14015–14020.
- Cooper G., and Rios A. C. 2016. Enantiomer excesses of rare and common sugar derivatives in carbonaceous meteorites. *Proceedings of the National Academy of Sciences* 113:E3322–E3331.
- Ehrenfreund P., and Charnley S. B. 2000. Organic Molecules in the Interstellar Medium, Comets, and Meteorites: A Voyage from Dark Clouds to the Early Earth. *Annual Review of Astronomy and Astrophysics* 38:427–483.
- Ehrenfreund P., Glavin D. P., Botta O., Cooper G., and Bada J. L. 2001. Extraterrestrial amino acids in Orgueil and Ivuna: Tracing the parent body of CI type carbonaceous chondrites. *Proceedings of the National Academy of Sciences of the United States of America* 98:2138–2141.
- Elsila J. E., Charnley S. B., Burton A. S., Glavin D. P., and Dworkin J. P. 2012. Compound-specific carbon, nitrogen, and hydrogen isotopic ratios for amino acids in CM and CR chondrites and their use in evaluating potential formation pathways. *Meteoritics and Planetary Science* 47:1517–1536.
- Elsila J. E., Aponte J. C., Blackmond D. G., Burton A. S., Dworkin J. P., and Glavin D. P. 2016. Meteoritic Amino Acids: Diversity in Compositions Reflects Parent Body Histories. *ACS Central Science* 2:370–379.
- Engel M. H., and Nagy B. 1982. Distribution and enantiomeric composition of amino acids in the Murchison meteorite. *Nature* 296:837–840.
- Furukawa Y., Chikaraishi Y., Ohkouchi N., Ogawa N. O., Glavin D. P., Dworkin J. P., Abe C., and Nakamura T. 2019. Extraterrestrial ribose and other sugars in primitive meteorites. *Proceedings of the National Academy of Sciences* 116:24440–24445.
- Glavin D. P., Bada J. L., Brinton K. L. F., and McDonald G. D. 1999. Amino acids in the Martian meteorite Nakhla. *Proceedings of the National Academy of Sciences* 96:8835–8838.
- Glavin D. P., Dworkin J. P., Aubrey A., Botta O., Doty J. H., Martins Z., and Bada J. L. 2006. Amino acid analyses of Antarctic CM2 meteorites using liquid chromatography-time of flight-mass spectrometry. *Meteoritics and Planetary Science* 41:889–902.
- Glavin D. P., and Dworkin J. P. 2009. Enrichment of the amino acid L-isovaline by aqueous alteration on CI and CM meteorite parent bodies. *Proceedings of the National Academy of Sciences of the United States of America* 106:5487–5492.

- Glavin D. P., Callahan M. P., Dworkin J. P., and Elsila J. E. 2010. The effects of parent body processes on amino acids in carbonaceous chondrites. *Meteoritics and Planetary Science* 45:1948–1972.
- Glavin D. P., Alexander C. M. O., Aponte J. C., Dworkin J. P., Elsila J. E., and Yabuta H. 2018. The Origin and Evolution of Organic Matter in Carbonaceous Chondrites and Links to Their Parent Bodies. In *Primitive Meteorites and Asteroids*. Elsevier. pp. 205–271.
- Glavin D. P. et al. 2020a. Abundant extraterrestrial amino acids in the primitive CM carbonaceous chondrite Asuka 12236. *Meteoritics & Planetary Science* 28:maps.13560.
- Glavin D. P., Elsila J. E., McLain H. L., Aponte J. C., Parker E. T., Dworkin J. P., Hill D. H., Connolly H. C., and Lauretta D. S. 2020b. Extraterrestrial amino acids and L-enantiomeric excesses in the CM2 carbonaceous chondrites Aguas Zarcas and Murchison. *Meteoritics & Planetary Science* 26:1–26.
- Gligorovski S., Strekowski R., Barbati S., and Vione D. 2015. Environmental Implications of Hydroxyl Radicals (\bullet OH). *Chemical Reviews* 115:13051–13092.
- Le Guillou C., Bernard S., Brearley A. J., and Remusat L. 2014. Evolution of organic matter in Orgueil, Murchison and Renazzo during parent body aqueous alteration: In situ investigations. *Geochimica et Cosmochimica Acta* 131:368–392.
- Guo W., and Eiler J. M. 2007. Temperatures of aqueous alteration and evidence for methane generation on the parent bodies of the CM chondrites. *Geochimica et Cosmochimica Acta* 71:5565–5575.
- Harju E. R., Rubin A. E., Ahn I., Choi B.-G., Ziegler K., and Wasson J. T. 2014. Progressive aqueous alteration of CR carbonaceous chondrites. *Geochimica et Cosmochimica Acta* 139:267–292.
- Howard K. T., Alexander C. M. O. D., Schrader D. L., and Dyl K. A. 2015. Classification of hydrous meteorites (CR, CM and C2 ungrouped) by phyllosilicate fraction: PSD-XRD modal mineralogy and planetesimal environments. *Geochimica et Cosmochimica Acta* 149:206–222.
- Kawasaki T., Hatase K., Fujii Y., Jo K., Soai K., and Pizzarello S. 2006. The distribution of chiral asymmetry in meteorites: An investigation using asymmetric autocatalytic chiral sensors. *Geochimica et Cosmochimica Acta* 70:5395–5402.
- Kebukawa Y., David Kilcoyne A. L., and Cody G. D. 2013. Exploring the potential formation of organic solids in chondrites and comets through polymerization of interstellar formaldehyde. *The Astrophysical Journal* 771:19.
- Kebukawa Y., Chan Q. H. S., Tachibana S., Kobayashi K., and Zolensky M. E. 2017.

- One-pot synthesis of amino acid precursors with insoluble organic matter in planetesimals with aqueous activity. *Science Advances* 3:e1602093.
- Kebukawa Y., Nakashima S., Mita H., Muramatsu Y., and Kobayashi K. 2020. Molecular evolution during hydrothermal reactions from formaldehyde and ammonia simulating aqueous alteration in meteorite parent bodies. *Icarus* 347:113827.
- Kimura M., Grossman J. N., and Weiserg M. K. 2011. Fe-Ni metal and sulfide minerals in CM chondrites: An indicator for thermal history. *Meteoritics & Planetary Science* 46:431–442.
- Koga T., and Naraoka H. 2017. A new family of extraterrestrial amino acids in the Murchison meteorite. *Scientific Reports* 7:1–8.
- Kvenvolden K. A., Lawless J. G., and Ponnampereuma C. 1971. Nonprotein Amino Acids in the Murchison Meteorite. *Proceedings of the National Academy of Sciences* 68:486–490.
- Lerner N. R., Peterson E., and Chang S. 1993. The Strecker synthesis as a source of amino acids in carbonaceous chondrites: Deuterium retention during synthesis. *Geochimica et Cosmochimica Acta* 57:4713–4723.
- Lerner N. R., and Cooper G. W. 2005. Iminodicarboxylic acids in the Murchison meteorite: Evidence of Strecker reactions. *Geochimica et Cosmochimica Acta* 69:2901–2906.
- Martins Z., Modica P., Zanda B., and D’Hendecourt L. L. S. 2015. The amino acid and hydrocarbon contents of the Paris meteorite: Insights into the most primitive CM chondrite. *Meteoritics & Planetary Science* 50:926–943.
- Matsuo Y., and Greenberg D. M. 1955. Metabolic formation of homoserine and alpha-aminobutyric acid from methionine. *The Journal of biological chemistry* 215:547–54.
- Naraoka H., and Hashiguchi M. 2019. Distinct distribution of soluble N-heterocyclic compounds between CM and CR chondrites. *Geochemical Journal* 53:33–40.
- Öberg K. I., Garrod R. T., van Dishoeck E. F., and Linnartz H. 2009. Formation rates of complex organics in UV irradiated CH₃OH-rich ices. *Astronomy & Astrophysics* 504:891–913.
- Orthous-Daunay F.-R., Quirico E., Lemelle L., Beck P., DeAndrade V., Simionovici A., and Derenne S. 2010. Speciation of sulfur in the insoluble organic matter from carbonaceous chondrites by XANES spectroscopy. *Earth and Planetary Science Letters* 300:321–328.
- Peltzer E. T., and Bada J. L. 1978. α -Hydroxycarboxylic acids in the Murchison

- meteorite. *Nature* 272:443–444.
- Peltzer E. T., Bada J. L., Schlesinger G., and Miller S. L. 1984. The chemical conditions on the parent body of the murchison meteorite: Some conclusions based on amino, hydroxy and dicarboxylic acids. *Advances in Space Research* 4:69–74.
- Pizzarello, S.; Cooper, G. W.; Flynn G. J. 2006. The Nature and Distribution of the Organic Material in Carbonaceous Chondrites and Interplanetary Dust Particles. *Meteorites and the Early Solar System II (Lauretta, D. S. and McSween, H. Y. Jr., Eds.), Univ. Arizona Press, Tucson, 625–651.*
- Pizzarello S., Zolensky M., and Turk K. A. 2003. Nonracemic isovaline in the Murchison meteorite: Chiral distribution and mineral association. *Geochimica et Cosmochimica Acta* 67:1589–1595.
- Pizzarello S., Huang Y., and Fuller M. 2004. The carbon isotopic distribution of Murchison amino acids. *Geochimica et Cosmochimica Acta* 68:4963–4969.
- Pizzarello S., and Huang Y. 2005. The deuterium enrichment of individual amino acids in carbonaceous meteorites: A case for the presolar distribution of biomolecule precursors. *Geochimica et Cosmochimica Acta* 69:599–605.
- Pizzarello S., Huang Y., and Alexandre M. R. 2008. Molecular asymmetry in extraterrestrial chemistry: Insights from a pristine meteorite. *Proceedings of the National Academy of Sciences* 105:3700–3704.
- Pizzarello S., Wang Y., and Chaban G. M. 2010. A comparative study of the hydroxy acids from the Murchison, GRA 95229 and LAP 02342 meteorites. *Geochimica et Cosmochimica Acta* 74:6206–6217.
- Pizzarello S., Williams L. B., Lehman J., Holland G. P., and Yarger J. L. 2011. Abundant ammonia in primitive asteroids and the case for a possible exobiology. *Proceedings of the National Academy of Sciences* 108:4303–4306.
- Pizzarello S., Schrader D. L., Monroe A. A., and Lauretta D. S. 2012. Large enantiomeric excesses in primitive meteorites and the diverse effects of water in cosmochemical evolution. *Proceedings of the National Academy of Sciences of the United States of America* 109:11949–11954.
- Pollock G. E., Cheng C.-N., Cronin S. E., and Kvenvolden K. A. 1975. Stereoisomers of isovaline in the Murchison meteorite. *Geochimica et Cosmochimica Acta* 39:1571–1573.
- Simkus D. N., Aponte J. C., Elsila J. E., Parker E. T., Glavin D. P., and Dworkin J. P. 2019. Methodologies for Analyzing Soluble Organic Compounds in Extraterrestrial Samples: Amino Acids, Amines, Monocarboxylic Acids, Aldehydes, and Ketones. *Life* 9:47.

- Smith K. E., House C. H., Arevalo R. D., Dworkin J. P., and Callahan M. P. 2019. Organometallic compounds as carriers of extraterrestrial cyanide in primitive meteorites. *Nature Communications* 10:1–7.
- Vollmer C., Pelka M., Leitner J., and Janssen A. 2020. Amorphous silicates as a record of solar nebular and parent body processes—A transmission electron microscope study of fine - grained rims and matrix in three Antarctic CR chondrites. *Meteoritics & Planetary Science* 18:maps.13526.
- Weisberg M. K., McCoy T. J., and Krot A. N. 2006. Systematics and Evaluation of Meteorite Classification. *Meteorites and the Early Solar System II (Lauretta, D. S. and McSween, H. Y. Jr., Eds.), Univ. Arizona Press, Tucson*, 19–52.
- Yanagawa H., Makino Y., Sato K., Nishizawa M., and Egami F. 1982. Novel Formation of α -Amino Acids and Their Derivatives from Oxo Acids and Ammonia in an Aqueous Medium. *The Journal of Biochemistry* 91:2087–2090.
- Yanagawa H., Makino Y., Sato K., Nishizawa M., and Egami F. 1984. Novel formation of α -amino acid from α -oxo acids and ammonia in an aqueous medium. *Origins of Life and Evolution of Biospheres* 14:163–169.
- Zhou Y., Quan D., Zhang X., and Qin S. 2020. Detection of hydroxyacetone in protostar IRAS 16293 – 2422 B *. *Research in Astronomy and Astrophysics*.

Supplementary Information

Table S1. Summary of the fragment ions (m/z) used for quantification of each HAA in the CM and CR chondrites.

	Y-791198		A-881458		LEW 90500		LON 94101		ALH 83100		MIL 07525		LAP 02342		MET 00426		GRO 95577	
	CM2 (CM2.4/1.6/1.5)		CM2, very weakly heated		CM2 (CM2.4/1.4/1.6)		CM2 (CM2.6/1.3/1.8)		CM1/2 (CM2.1/1.2/1.1)		CR2 (CR2.8)		CR2 (CR2.8/2.7/2.5)		CR2 (CR2.8/2.6/2.6)		CR1 (CR2.0/1.3/1.3)	
Hydroxy amino acids (Peak # in Fig. 1-3 & 1-4)	HW	HCl	HW	HCl	HW	HCl	HW	HCl	HW	HCl	HW	HCl	HW	HCl	HW	HCl	HW	HCl
D-Serine (#1)	239	239	239	239	239	239	239	239	239	239	239	239	239	239	239	239	239	239
L-Serine (#2)	239	239	284	239	239	239	239	239	239	239	239	239	239	239	239	239	239	239
DL-Isoserine (#3 & 4)	452	239	239	239	239	452	239	452	452	239	239	239	452	452	239	452	239	239
L- α -Methylserine (#5)	252	252	252	252	252	252	252	252	252	252	252	252	252	252	252	252	252	252
D- α -Methylserine (#6)	252	252	252	252	252	252	252	252	252	252	252	252	252	252	252	252	252	252
D-Threonine (#7)	253	253	253	253	253	253	253	253	n.d.	n.d.	253	253	253	253	253	253	n.d.	n.d.
L-Threonine (#8)	253	253	253	253	253	253	253	253	253	253	253	253	253	253	253	253	253	253
Isothreonine (#9)	466	466	466	466	466	466	466	466	n.d.	n.d.	466	466	466	466	466	466	n.d.	n.d.
Isothreonine (#10)	466	466	466	466	466	466	466	466	n.d.	n.d.	466	466	466	466	466	466	n.d.	n.d.
DL- α -Methylisoserine (#11)	466	252	466	252	252	466	252	466	252	252	466	466	466	466	466	466	252	252
D- <i>allo</i> -Threonine (#12)	253	253	253	253	253	253	253	253	253	253	466	298	238	253	466	252	n.d.	n.d.
L- <i>allo</i> -Threonine (#13)	253	253	253	253	253	253	253	253	253	253	466	298	238	253	466	252	n.d.	n.d.
<i>allo</i> -Isothreonine (#14)	272	466	272	272	272	272	272	272	n.d.	272	272	272	272	272	272	272	n.d.	n.d.
<i>allo</i> -Isothreonine (#15)	272	466	272	272	272	272	272	272	n.d.	272	272	272	272	272	272	272	n.d.	n.d.
D-Homoserine (#16)	252	252	298	252	252	252	252	252	252	252	252	252	252	252	252	252	252	252
L-Homoserine (#17)	252	252	298	252	252	252	252	252	252	252	252	252	252	252	252	252	252	252
DL- β -Homoserine (#18)	494	494	494	n.d.	494	494	494	494	494	n.d.	494	494	494	494	494	494	n.d.	n.d.
D-3-A-2-HMPA (#19)	280	280	280	280	n.d.	280	n.d.	280	n.d.	n.d.	n.d.	280	n.d.	280	n.d.	280	n.d.	n.d.
L-4-A-2-HBA (#20)	466	466	466	466	n.d.	466	n.d.	466	n.d.	466	n.d.	466	n.d.	466	n.d.	466	466	466
D-4-A-3-HBA (#21)	252	252	280	252	n.d.	252	n.d.	252	n.d.	252	n.d.	280	n.d.	252	n.d.	280	252	n.d.
L-4-A-3-HBA (#22)	252	252	280	252	n.d.	252	n.d.	252	n.d.	252	n.d.	280	n.d.	252	n.d.	280	252	n.d.

n.d. = value not determined due to trace amino acid abundance.